Robust Mask-Based Appointment Scheduling in Primary Care Practices

Sabrina Schmitz   Martin Comis   Christina Büsing

December 7, 2023

Abstract

In most health care systems, a primary care physician (PCP) is both the first instance consulted by patients with medical concerns and the instance coordinating patients' continued access to medical care. Due to the PCP's pivotal role, we address challenges of a high-quality primary care service by interday appointment scheduling on a tactical decision level. Our study considers three different types of patients, including walk-ins who complicate the PCP's schedule planning as they forgo scheduling an appointment and seek immediate care by walking into the practice without prior notice. We study appointment scheduling systems based on so-called masks and focus on the balanced workload of the PCP in form of the mask design problem. To account for different uncertainties in demand for treatment, we extend the mask design problem to the robust mask design and the robust multimask design problem. For all three problems, we provide a combinatorial interpretation by a network flow and design model. We develop a solution approach that combines binary search with compact formulations (of extensions) of minimum cost flow problems. Finally, we conduct an extensive case study by agent-based simulation in which we evaluate the mask-based appointment scheduling systems and compare them with five appointment scheduling systems from the literature.

1 Introduction

Primary care physicians (PCPs) play a crucial role in health care systems as they are often the first instance consulted by patients with medical concerns [7, 22]. PCPs' responsibilities begin with conducting an examination to determine the patients' states of health and assessing whether they themselves can provide the necessary medical care. If this is not the case, they are obliged to ensure the continuation of medical care, for example by referring the patient to a specialist [43]. As the instance facilitating and coordinating patients' access to medical care, the PCP's quality of service is not only measured on the basis of competent medical care but also by aspects such as the patient-physician continuity, timely access to medical care, and waiting times within the practice, as discussed in more detail in the following.

Patient-physician continuity is desirable as patients benefit from follow-up treatments and referrals [4, 43]. PCPs themselves benefit as they have to spend less time dealing with medical histories of new patients [22]. Clearly, patient-physician continuity may conflict with swift access to health care if patients prefer to be treated by their familiar

PCP rather than by any available PCP [6]. Timely access to medical care is imperative, as it is decisive for the patients' choice of medical facility, course of illness, and medical outcome [22, 55]. For instance, long access times for PCP practices increase the likelihood of patients visiting emergency rooms [50, 44].

In the United States, patients' timely access is endangered by the clash of increasing demand for primary health care and the nationwide lack of PCPs [7, 38]. Similar conflicts arise in other countries. In rural areas of Germany, the prospect of timely medical care is at risk due to mainly elderly PCPs near retirement [5] combined with fewer medical graduates who are willing to start a practice [29]. Due to the worldwide aging population at the highest risk of chronic conditions [38, 3], PCPs' schedules are already overloaded [10]. Overloading in turn results in long waiting times in the practice—one of the major reasons for patients' complaints [25].

To face the described and further challenges of high-quality service, an effective appointment scheduling system is required [23, 40]. However, the PCPs' schedule planning is complicated as patients forgo scheduling an appointment and seek immediate care by walking into the practice without prior notice—as so-called walk-ins. Over the past ten years, German surveys conducted by The National Association of Statutory Health Insurance Physicians [42] reveal that on average 18.8% of the patients forgo scheduling an appointment and are seen by their PCP as walk-in. Compared to specialists with an average rate of 6.5%, this almost three times higher rate highlights the difficulty of the scheduling in primary care practices. The scheduling is further complicated by fluctuating demand for treatment which leads to an inefficient and imbalanced workflow of PCPs [54]. PCPs have to work overtime on one day and are underutilized on another day of the same week. In summary, an effective appointment scheduling system maintains patient-physician continuity, enables timely access, reduces waiting times, smooths the PCP workflow, and provides robustness against demand uncertainties [22].

The main contributions of this paper are summarized as follows. Considering three different types of patients, we manage a PCP's demand for treatment by interday appointment scheduling on a tactical decision level. For this purpose, we first formalize appointment scheduling systems that preserve an efficient and balanced workflow of the PCP by the so-called mask design problem (MDP) in a deterministic setting. We provide a combinatorial interpretation of the MDP by a network flow and design model. For this model, we present a solution approach that combines binary search and compact integer program (IP) formulations of minimum cost flow problems. We extend the MDP to a robust setting due to uncertainties in demand for treatments and provide the resulting robust mask design problem (rMDP). In addition, to account for further uncertainties in demand for treatment and overfitted solutions, we present the robust multimask design problem (rMMDP). For the rMDP and rMMDP, we extend our solution approach by robust compact minimum cost flow formulations. Based on the solutions to the MDP, rMDP, and rMMDP, we obtain so-called mask-based appointment scheduling systems. We conduct an extensive case study using agent-based simulation. In this case study, we evaluate the mask-based appointment scheduling systems and compare them with five appointment scheduling systems from the literature. We can observe that especially the robust mask-based appointment scheduling systems leads to high-quality solutions in several key performance indicators. To the best of our knowledge, this is the first contribution that studies (interday) appointment scheduling by means of combinatorial and robust methods. More precisely, this is the first contribution that studies (interday)

appointment scheduling as a (robust) network flow and design problem.

The paper is structured as follows. In Section 2, we outline literature of appointment scheduling in primary health care with a focus on interday appointment scheduling. In Section 3, we define a physician-patients setting, introduce mask-based interday appointment scheduling, and present the mask design problem. In Section 4, we model the mask design problem in a deterministic setting and subsequently extend it to a robust setting. In Section 5, we consider the extension of the mask design problem, the multimask design problem. We note that the modeling in Sections 4 and 5 is presented step-by-step in great detail. In Section 6, we present and discuss the results from our case study. In Section 7, we discuss and conclude our results.

2 Appointment scheduling in the literature

Health care services face many challenges due to the clash of increasing demand for medical care and the resources available [9, 14]. In the overview [27], Hulshof et al. identify the general classifications of planning and control decisions of health care services. Concentrating on appointment scheduling in outpatient services, we refer to the overview of Cayirli and Veral [12] which focuses on formulating general problems and their various modelings. Factors that make appointment scheduling challenging are demonstrated by Gupta and Denton [22]. Furthermore, we refer to Ahmadi-Javid et al. [2] for a review of analytical and numerical optimization studies for outpatient appointment scheduling systems. In the following, we provide an overview about the categories into which appointment scheduling systems are classified as well as related work.

2.1 Categories of appointment scheduling systems

Appointment scheduling systems established in the literature are categorized into four different types of systems [53]: traditional, advanced access, hybrid, and carve-out appointment scheduling systems. The traditional appointment scheduling system allows all slots to be scheduled for appointments by requesting patients. Appointments may be scheduled well in advance and are often used to postpone patients requests. In contrast, the advanced access appointment scheduling system accommodates all patients on the day of their request. The core idea is to schedule same-day appointments only [40]. Robinson and Chen [49] compare these two contrasting scheduling policies regarding various performance measures. Both appointment scheduling systems show a lack of planning security with respect to the actual number of treatments. The traditional appointment scheduling system is disadvantageous for two reasons: short-term cancellations and no-shows, i.e., patients who do not show up for their appointments. Overbooking strategies have been proven to reduce the resulting negative impacts [13, 26, 31, 36, 37, 49, 56]. Further difficulties for the traditional appointment scheduling system are, for example, long access times to appointments and insufficient time for (walk-in) patients with acute or urgent concerns [48]. The advanced access appointment scheduling system becomes less efficient due to the uncertain demand for treatment. This causes waiting times for patients as well as inefficient and imbalanced working hours for PCPs [49]. The request for appointments scheduled in advance is also not considered, which particularly affects elderly and chronically ill patients [2, 53]. Furthermore, on days with high demand for treatment patients are still referred to the next session or the following day—the so-called overflow patients.

Thus, same-or-next-day scheduling policies also appear in the context of advanced access systems [40] which have been proven to be successful against simple same-day scheduling policies [49]. For this reason, hybrid appointment scheduling systems are introduced that combine the two concepts [13, 47, 49]. Finally, the carve-out appointment scheduling system is managed as the traditional appointment scheduling system where a part of the PCP's working hours is reserved for specific procedures or urgent services [2, 53]. We note that the categorization of appointment scheduling systems becomes blurred as the systems overlap. In addition, the categorization is not clearly defined due to different assumptions, settings, services, and facilities of various health care systems of different countries.

Besides the differentiation in appointment scheduling systems, studies are further categorized according to intraday and interday appointment scheduling [19]. Intraday appointment scheduling concentrates on a single day with emphasis on, for example, the reduction of patient waiting times or the patient-physician continuity. In this context, mostly same-day scheduling policies are investigated on tactical and operational decision levels. In contrast, the concept of interday appointment scheduling aims at allocating appointments for consecutive days to manage the PCP's working hours, usually on a tactical decision level. Fluctuating demand for treatment is smoothed throughout the week, and therefore, the utilization of the PCP's working hours and patient arrivals are controlled in a more efficient way.

In this study, we analyze an appointment scheduling system that analogously operates to a carve-out system. Appointments are traditionally scheduled while ample time is reserved for walk-ins to serve their urgent needs. For designing an appointment scheduling system, we refer to studies [21, 24] that introduce a notion similar to ours. As we focus on interday appointment scheduling in this study, we propose further related literature in the following section.

2.2 Related work

Qu et al. [46] manage a hybrid appointment scheduling system by a two time horizon. The first time horizon is used to schedule same-day appointments and the second to postpone demand for treatment within a maximum of one week. Regarding the expectation and variance of the number of patients seen by the PCP, the authors show that the two time horizon system is at least as good as an advanced access appointment scheduling system. Further, Qu et al. [48] investigate the ratio between same-day appointments and appointments in advance by an analytical method with the aim of maximizing the expected number of treated patients. The results show the important dependency of the average demand for same-day appointments to the PCP's working hours. Dobson et al. [18] formulate a stochastic model to determine the optimal number of slots reserved for urgent patients. They compare the resulting carve-out appointment scheduling system with an advanced access appointment scheduling system on the basis of revenue, i.e., the average number of urgent patients who are not seen during the PCP's working hours and the average queue length for routine patients. Feldman et al. [19] develop a dynamic appointment scheduling model that considers not only appointment cancellations and no-shows but also patients' preferences. If appointments do not match their preferences, patients are not seen by the PCP. Thus, Feldman et al. aim at a maximum expected revenue per day determined by patients treated.

In contrast to these studies, like Wiesche et al. [54], we consider patients with acute concerns who attempt scheduling an appointment within their willingness to wait. If no appointment is proposed within this time, they forgo scheduling an appointment and become walk-ins. Wiesche et al. [54] determine the minimum number of appointments scheduled for a weekly profile to match capacity with demand by a mixed integer program formulation. Stochastic simulation shows that their appointment scheduling strategy balances the PCP's work hours and reduces overflow patients. Schacht [51] extends the contributions by seasonal and stochastic aspects. He concludes that reconfiguration of the PCP's working hours throughout the year is advantageous. Unlike studies of Wiesche et al. [54] and Schacht [51], we do not minimize the number of appointment slots to have as much capacity as possible for walk-ins. Instead, we intend to offer appointment slots, motivated by the German health care system where only three percent of all primary care practices do not offer appointments [42]. More precisely, we aim at determining an optimal ratio between appointment slots and reserved time for walk-ins. We also note that, unlike studies [54] and [51], we do not neglect patients whose demand for treatment is known well in advance, for instance as it is the case for chronically ill patients. Instead, we use this controllable demand to manage and balance the PCP's workload.

The key difference between previously published studies and ours is that we use combinatorial optimization and do not consider stochastic but robust optimization models. To the best of our knowledge, we are the first who use combinatorial and robust solving methods to develop an appointment scheduling system.

3 Setting and problem definition

In this section, we introduce notations and formalize the appointment scheduling problem. In Section 3.1, we introduce a deterministic physician-patients setting. In Section 3.2, we show how to control demand for treatment by masked-based interday appointment scheduling. In Section 3.3, we present the MDP.

3.1 Deterministic physician-patients setting

Like most studies on primary health care [2], our study assumes a *single-server system*, i.e., practices with one PCP, because of the importance of patient-physician continuity. The single-server assumption holds even in joint practices, as PCPs usually provide medical care to their own panel of patients [12, 41]. PCPs generally operate in clinical sessions—a morning and an afternoon session. We denote the set of all sessions by $\mathcal{K}$. Concentrating on a single working week, we describe each *session* by a tuple $k = (i, j) \in \mathcal{K}$, where $i \in \{0, \ldots, 4\}$ indicates the working day from Monday to Friday and a binary indicator $j \in \{0, 1\}$ represents whether the morning ($j = 0$) or afternoon ($j = 1$) session is considered. For each of these sessions, we refine the PCP's working hours by differentiating between opening hours, buffer time, and overtime. *Opening hours* determine the time span $\boldsymbol{o} \in \mathbb{Z}_{\geq 0}^{\mathcal{K}}$ in which appointments are scheduled and patients may be admitted for treatments. After opening hours, we assume PCPs to use *buffer time* $\boldsymbol{b} \in \mathbb{Z}_{\geq 0}^{\mathcal{K}}$ to compensate for contingencies such as delays. We refer to the time during the start of the opening hours and the end of the buffer as the PCP's *capacity*, denoted by parameter $\boldsymbol{c} := \boldsymbol{o} + \boldsymbol{b}$. PCPs who do *overtime* work even beyond the buffer time. Figure 1 illustrates an exemplary working day of a PCP who operates in two sessions.
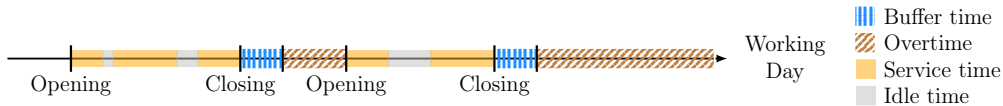
Figure 1: Schematic representation of a PCP's morning and afternoon session visualizing buffer, idle time, and overtime

During the PCP's opening hours, patients have two options to seek medical care in the modeled setting—either by appointment or as walk-in. Whether patients first contact their PCP or accept a proposed appointment depends on their *willingness to wait* which varies with their health status. In this context, we divide patients into three categories: *walk-ins*, *regular*, and *chronic patients*. The last suffer from chronic illnesses and seek follow-up treatments by appointment. We assume that their willingness to wait ensures flexibility in their appointment requests and we therefore specify their demand as a single weekly demand $d^c \in \mathbb{Z}_{\geq 0}$. In contrast, regular patients suffer from acute illnesses and request an appointment for a specific session, specified by demand $\boldsymbol{d}^r \in \mathbb{Z}_{\geq 0}^{\mathcal{K}}$. If they are not offered an appointment in this session or an alternative appointment within their willingness to wait, regular patients forgo an appointment and seek immediate care as walk-ins in the session of their request. Motivated by German employees, who must provide a sick note after three days of sick leave [17], we uniformly set their willingness to wait to three days. Naturally, there always exist some additional walk-ins who are not willing to wait at all and who do not even request an appointment. We specify their demand per session by parameter $\boldsymbol{d}^w \in \mathbb{Z}_{\geq 0}^{\mathcal{K}}$.

Once patients request to be treated, the treatments' duration are naturally subject to variation. Nevertheless, studies have shown that the length of the treatments only marginally varies in primary care [39, 52]. Thus, we assume a uniform *anticipated service time* $t \in \mathbb{Z}_{>0}$ for all patients.

Before proposing a method to manage patient demand, we note that our models generalize to finer demand aggregations, for example, for every 30 minutes of a session. However, as our models support on a tactical decision level and as some of the models are based on a single demand realization, finer aggregations may lead to overfitting and consequently to appointment scheduling systems that are not generally applicable.

3.2 Controlling patient demand by masked-based interday appointment scheduling

Naturally, patient demand is unevenly distributed over the sessions within a week. Therefore, we manage controllable demand and consider potential uncontrollable demand by interday appointment scheduling. More precisely, we beneficially distribute chronic demand d^c over the week while we shift regular demand $\boldsymbol{d}^r$ from days with high demand to days with lower demand. Following this strategy, we account for the walk-in demand $\boldsymbol{d}^w$ which is not controllable by postponement to a later session. To address this issue, we employ a cyclic model of a single working week. We assume that the regular demand which is shifted to the following week due to scheduled appointments, e.g., from Friday to Monday, compensate for the regular demand that would, theoretically, be shifted from the previous week. To shift (part of) the regular demand d_k^r, $k \in \mathcal{K}$ to an alternative session that is within the patient's willingness to wait, we define a set of all feasible sessions as

follows

$$\mathcal{K}^+_{k=(i,j)} = \left\{ \; k' = (i', j') \in \mathcal{K} \; \middle| \; (i' - i) \bmod 5 \leq 2, \; o_{k'} > 0 \; \right\}.$$

For later purposes, we define a set to summarize the sessions originally have been requested by regular patients alternatively scheduled in session $k \in \mathcal{K}$ as follows

$$\mathcal{K}^-_{k=(i,j)} = \left\{ \; k' = (i', j') \in \mathcal{K} \; \middle| \; -(i' - i) \bmod 5 \leq 2, \; o_{k'} > 0 \; \right\}.$$

Using these sets, we formalize the distribution of the chronic demand and the shifts of the regular demand in the following definition.

Definition 1 (Assignment). Let demands $d^c \in \mathbb{Z}_{\geq 0}$ and $\boldsymbol{d}^r \in \mathbb{Z}^{\mathcal{K}}_{\geq 0}$ be given. A $(d^c, \boldsymbol{d}^r)$-*assignment* $\boldsymbol{\alpha} = (\alpha^c, \boldsymbol{\alpha}^r) = (\alpha^c, \alpha^r_{(0,0)}, \ldots, \alpha^r_{(4,1)})$ is a $(|\mathcal{K}| + 1)$-tuple of functions $\alpha^c : \mathcal{K} \to \mathbb{Z}_{\geq 0}$ and $\alpha^r_k : \mathcal{K}^+_k \to \mathbb{Z}_{\geq 0}$, $k \in \mathcal{K}$ that distribute and shift the demand across sessions, respectively, such that $\sum_{k \in \mathcal{K}} \alpha^c(k) = d^c$ and $\sum_{k' \in \mathcal{K}^+_k} \alpha^r_k(k') \leq d^r_k$, $k \in \mathcal{K}$ holds.

Considering the definition of an assignment, we note the following three aspects. First, an assignment has to distribute the entire chronic demand d^c and may not shift more than the regular demand d^r_k of each session $k \in \mathcal{K}$. Second, whenever a regular patient is assigned by function $\boldsymbol{\alpha}^r$ to the requested or a later occurring session, we assume the patient to see the PCP by appointment. Conversely, this means that the number of regular patients who are not assigned, i.e., $d^r_k - \sum_{k' \in \mathcal{K}^+_k} \alpha^r_k(k')$, determines the number of regular patients who become walk-ins in session $k \in \mathcal{K}$. Third, assignments do not have to respect the PCP's capacity by definition and thus may lead to overtime. For this reason, we strive for a system by which demand is reasonably assigned—in other words, an appointment scheduling system.

In primary care practices, appointment scheduling systems are usually based on time slots. To implement time slots in our setting, we divide the time span o_k of the PCP's opening hours for each session $k \in \mathcal{K}$ into time periods of equal length $\ell \in \mathbb{Z}_{>0}$. Each *slot* is described by a tuple $s = (k, q_k)$ where $k \in \mathcal{K}$ indicates the session and $q_k \in \{1, \ldots, n_k\}$ with $n_k := \lceil \frac{o_k}{\ell} \rceil \in \mathbb{Z}_{\geq 0}$ the position. We denote the set of all slots within the weekly PCP's capacity by $\mathcal{S}$. We assume one scheduled patient per slot and, in order to reserve a reasonable amount of time, we require the slot length ℓ to be at least as long as the anticipated service time t, i.e., $\ell \geq t$. Figure 2 visualizes an exemplary schedule of a five-day working week with ten-minute slots where the PCP's practice is closed on Wednesday and Friday afternoons.

At this point, we allow slots to have one of the following three *states*: chronic c, regular r and walk-in w. States are supposed to indicate whether a slot is reserved to schedule a chronic or regular patient or whether a slot is reserved for a potential walk-in. For simplicity's sake, we refer to slots with state 'chronic', 'regular', and 'walk-in' also as chronic, regular, and walk-in slots. Using the states of slots, we can define a mask.

Definition 2 (Mask). A *mask* is a function $\mu : \mathcal{S} \to \{c, r, w\}$ that assigns each slot one state.

In the following, we assign demand, or in other words, schedule appointments on the basis of a mask. Since masks regulate how many chronic and regular patients may be scheduled and how many slots are reserved for potential walk-ins, assignments need to be compatible.

Figure 2: Schedule defined by consecutive slots

Definition 3 ($\boldsymbol{\alpha}$-compatible mask). Mask μ and $(d^c, \boldsymbol{d}^r)$-assignment $\boldsymbol{\alpha} = (\alpha^c, \boldsymbol{\alpha}^r)$ are *compatible* with each other if $\boldsymbol{\alpha}$ assigns at most as much chronic and regular demand as chronic and regular slots are available, respectively, i.e., for $k \in \mathcal{K}$ it holds

$$\alpha^c(k) \leq n_\mu(c, k) = |\{s = (k, q_k) \in \mathcal{S} \mid \mu(s) = c\}|,$$

$$\sum_{k' \in \mathcal{K}_k^-} \alpha_{k'}^r(k) \leq n_\mu(r, k) = |\{s = (k, q_k) \in \mathcal{S} \mid \mu(s) = r\}|.$$

The set of all $(d^c, \boldsymbol{d}^r)$-assignments that are compatible with mask μ is denoted by $\mathcal{A}^\mu$. If $\boldsymbol{\alpha} \in \mathcal{A}^\mu$ holds, we say a mask μ is $\boldsymbol{\alpha}$-*compatible*.

Overall, we obtain an appointment scheduling system based on a mask and compatible assignments referred to as *mask-based appointment scheduling system*. In the next section, we design a mask that aims at a balanced utilization of the capacity of the PCP. We note that masks can be designed according to different objectives such as the distribution of certain types of patients to certain working days.

3.3 Balanced utilization by the MDP

A main goal PCPs strive for is an efficient workflow. This includes a balanced workload to avoid PCPs working overtime on one day while not working at full capacity on another day of the same week. To achieve this in our setting on a tactical decision level, we strive for a balanced use of the weekly capacity. We start with formal definitions for the workload per session, the weekly utilization, and the, in terms of a balanced utilization of the weekly capacity, optimal workload per session.

Given demands $d^c \in \mathbb{Z}_{\geq 0}$ and $\boldsymbol{d}^r, \boldsymbol{d}^w \in \mathbb{Z}_{\geq 0}^{\mathcal{K}}$ as well as a $(d^c, \boldsymbol{d}^r)$-assignment $\boldsymbol{\alpha}$, we define the PCP's *workload* $\Phi_k(\boldsymbol{\alpha}, d_k^w)$ in session $k \in \mathcal{K}$ by the anticipated working time resulting from all treatments requested in and assigned to session k, i.e.,

$$\Phi_k(\boldsymbol{\alpha}, d_k^w) = \left(d_k^w + d_k^r - \sum_{k' \in \mathcal{K}_k^+} \alpha_k^r(k') + \sum_{k' \in \mathcal{K}_k^-} \alpha_{k'}^r(k) + \alpha^c(k) \right) t.$$

We note that the PCP's workload depends on demands and assignments. Recalling the cyclic model and using the weekly patient demand, we can compute the *weekly utilization*

8

u of the PCP by

$$u = \frac{t}{C}\left(d^c + \sum_{k\in\mathcal{K}}(d_k^r + d_k^w)\right),$$

where $C = \sum_{k\in\mathcal{K}} c_k$ denotes the PCP's weekly capacity. We obtain the, in terms of balance, *optimal workload* per session as the product of the weekly utilization and the session's capacity, i.e., $u \cdot c_k$ for $k \in \mathcal{K}$. As the PCP's workload depends on assignments and the assignments in turn are restricted by masks, we can manage the PCP's workload by the design of a mask. Aiming at an optimal workload in every session, we evaluate masks according to the achievable workload balance.

Definition 4. Let the PCP's capacity $\boldsymbol{c} \in \mathbb{Z}_{\geq 0}^{\mathcal{K}}$ and demands $d^c \in \mathbb{Z}_{\geq 0}$, $\boldsymbol{d}^r, \boldsymbol{d}^w \in \mathbb{Z}_{\geq 0}^{\mathcal{K}}$ be given. We define the *cost* of a mask μ as the maximum deviation of the actual from the optimal workload among all sessions, provided that the workload is subject to a $(d^c, \boldsymbol{d}^r)$-assignment $\boldsymbol{\alpha} \in \mathcal{A}^\mu$ that minimizes the cost, i.e.,

$$c(\mu) = \min_{\boldsymbol{\alpha}\in\mathcal{A}^\mu} \max_{k\in\mathcal{K}} |\Phi_k(\boldsymbol{\alpha}, d_k^w) - u \cdot c_k|.$$

We conclude this section with the definition of the MDP.

Definition 5 (MDP). Given the PCP's capacity $\boldsymbol{c} \in \mathbb{Z}_{\geq 0}^{\mathcal{K}}$ and demands $d^c \in \mathbb{Z}_{\geq 0}$, $\boldsymbol{d}^r, \boldsymbol{d}^w \in \mathbb{Z}_{\geq 0}^{\mathcal{K}}$, the *mask design problem* aims at a mask of minimum cost.

4 Modeling the MDP

In this section, we present an extensive combinatorial interpretation of the MDP by a network flow and design model. First, we consider a model in a deterministic setting and subsequently extend this model to a robust setting.

4.1 MDP in a deterministic setting

In this section, we model the MDP by a network flow and design formulation. For this purpose, we construct a network in which a PCP's patient flow is modeled. An exemplary network of a five-day working week with one session per day is visualized in Figure 3. The network is defined by an acyclic digraph $G = (V, A)$ with vertex set V and arc set A. Besides auxiliary vertices v_k^1 and v_k^2 for all $k \in \mathcal{K}$, vertex set V includes multiple sources and a single sink that represent the patient demand. More precisely, let $\sigma^c \in V$ be the source that models the weekly chronic demand and let $\sigma_k^r \in V$ and $\sigma_k^w \in V$ be the sources that model the regular and walk-in demand per session $k \in \mathcal{K}$, respectively. Let $\tau \in V$ be the unique sink which ensures that all patients are seen by the PCP. A flow originating from one of the sources only reaches the sink by using at least one of two kind of arcs. The first type of arcs $a_k^1 = (v_k^1, \sigma_k^w) \in A$ represents regular and chronic patients scheduled in session $k \in \mathcal{K}$ referred to as appointment arcs. To limit the number of patients scheduled, we define upper arc capacities $\overline{\psi} : A \to \mathbb{Z}_{\geq 0}$ on the appointment arcs that are equal to the number of slots of the PCP's opening hours, i.e., $\overline{\psi}(a_k^1) = n_k$ for all $k \in \mathcal{K}$. As regular patients may be scheduled within three days after their requests, we add arcs that connect source σ_k^r, $k \in \mathcal{K}$ with the tail of the appointment arcs, i.e., with vertices $v_{k'}^1 \in V$ for
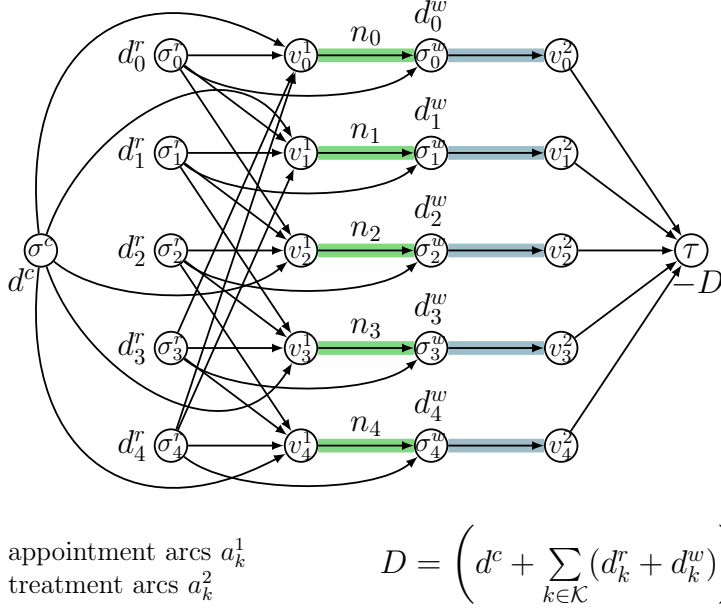
Figure 3: Network flow model for managing patient flow

$k' \in \mathcal{K}_k^+$. Furthermore, as chronic patients may be scheduled for each session, source σ^c is also connected with vertex v_k^1 for all $k \in \mathcal{K}$. The second type of arcs $a_k^2 = (\sigma_k^w, v_k^2) \in A$ represents all patients seen by the PCP in session $k \in \mathcal{K}$ referred to as treatment arcs. Accordingly, the treatment arc a_k^2 is connected in series with the appointment arc a_k^1 of the same session $k \in \mathcal{K}$. We note that the connection vertex is the source $\sigma_k^w \in V$ that models the walk-in demand in session $k \in \mathcal{K}$. In addition, source σ_k^r, $k \in \mathcal{K}$ is also connected with the connection vertex σ_k^w, i.e., with the tail of treatment arc a_k^2, which models regular patients who become walk-ins. Finally, each treatment arc a_k^2, $k \in \mathcal{K}$ is connected with sink τ. For all vertices $v \in V$, balances $\beta : V \to \mathbb{Z}$ with $\sum_{v \in V} \beta(v) = 0$ are defined as follows

$$\beta(v) = \begin{cases} d_k^r & \text{if } v = \sigma_k^r,\ k \in \mathcal{K}, \\ d_k^w & \text{if } v = \sigma_k^w,\ k \in \mathcal{K}, \\ d^c & \text{if } v = \sigma^c, \\ -\left(d^c + \sum_{k \in \mathcal{K}}(d_k^r + d_k^w)\right) & \text{if } v = \tau, \\ 0 & \text{otherwise.} \end{cases}$$

Overall, we obtain network $N = (G, \overline{\psi}, \beta)$.

In network N, a feasible integral β-flow is defined by a function $f : A \to \mathbb{Z}_{\geq 0}$ that satisfies the flow balance constraints $\sum_{a=(v,w) \in A} f(a) - \sum_{a=(w,v) \in A} f(a) = \beta(v)$ at every vertex $v \in V$ and the capacity constraints $0 \leq f(a_k^1) \leq \overline{\psi}(a_k^1)$ on all appointment arcs $a_k^1 \in A$. We note that all flows in this study are integrally defined. A β-flow in network N corresponds to a feasible solution to the MDP as shown in the following lemma.

Lemma 1. Let f be a feasible β-flow in network N. Flow f defines

(1) a $(d^c, \boldsymbol{d}^r)$-assignment $\boldsymbol{\alpha} = (\alpha^c, \boldsymbol{\alpha}^r)$ with $\alpha^c(k) = f((\sigma^c, v_k^1))$ and $\alpha_k^r(k') = f((\sigma_k^r, v_{k'}^1))$ and

(2) a mask $\mu : \mathcal{S} \to \{c, r, w\}, s = (k, q_k) \mapsto \mu(s)$ with

$$\mu(s) = \begin{cases} c & \text{if } q_k \in \{1, \dots, f((\sigma^c, v_k^1))\}, \\ r & \text{if } q_k \in \{f((\sigma^c, v_k^1)) + 1, \dots, f(a_k^1)\}, \\ w & \text{otherwise.} \end{cases}$$

that are compatible with each other.

Proof. First, flow f defines a feasible $(d^c, \boldsymbol{d}^r)$-assignment $\boldsymbol{\alpha} = (\alpha^c, \boldsymbol{\alpha}^r)$ due to the flow balance constraints as shown in the following expression

$$\sum_{k \in \mathcal{K}} \alpha^c(k) = \sum_{k \in \mathcal{K}} f((\sigma^c, v_k^1)) = d^c,$$

$$\sum_{k' \in \mathcal{K}_k^+} \alpha_k^r(k') = \sum_{k' \in \mathcal{K}_k^+} f((\sigma_k^r, v_{k'}^1)) \leq d_k^r, \ k \in \mathcal{K}.$$

Second, flow f defines a feasible mask μ as each slot is assigned exactly one state. We note that the arc capacities ensure that no more slots are assigned a status by the flow than there exist slots in the mask, i.e., it holds $q_k \leq f(a_k^1) \leq \overline{\psi}(a_k^1) = n_k$ for $k \in \mathcal{K}$. Assignment $\boldsymbol{\alpha}$ and mask μ are compatible as $\alpha^c(k) = f((\sigma^c, v_k^1)) = n_\mu(c, k)$ and $\sum_{k' \in \mathcal{K}_k^-} \alpha_{k'}^r(k) = \sum_{k' \in \mathcal{K}_k^-} f((\sigma_{k'}^r, v_k^1)) = f(a_k^1) - f((\sigma^c, v_k^1)) = n_\mu(r, k)$ hold for every $k \in \mathcal{K}$. $\square$

We recall that the flow value on the treatment arc a_k^2 represents the number of patients seen by the PCP in session $k \in \mathcal{K}$. So, multiplying this number by the anticipated service time t results in the PCP's workload in session $k \in \mathcal{K}$. Thus, to obtain an optimal solution to the MDP, we aim at a feasible β-flow f in network N that minimizes the following expression

$$\max_{k \in \mathcal{K}} |t \cdot f(a_k^2) - u \cdot c_k|. \tag{1}$$

In other words, we look for a flow that is balanced on the treatment arcs. To determine such a flow, we add lower and upper arc capacities $\underline{\psi}_\omega, \overline{\psi}_\omega : A \to \mathbb{Z}_{\geq 0}$ for a parameter $\omega \in \mathbb{Z}_{\geq 0}$ on the treatment arcs $a_k^2 \in A, k \in \mathcal{K}$ of network N. We denote the resulting network by $N_\omega = (G, \overline{\psi}, \underline{\psi}_\omega, \overline{\psi}_\omega, \beta)$. The lower and upper arc capacities are defined such that the PCP's actual workload in session $k \in \mathcal{K}$ may deviate from the optimal workload $u \cdot c_k$ by an amount of $\omega \in \mathbb{Z}_{\geq 0}$, i.e., $\underline{\psi}_\omega(a_k^2) = \max \left\{ \left\lceil \frac{1}{t} (u \cdot c_k - \omega) \right\rceil, 0 \right\}, \overline{\psi}_\omega(a_k^2) = \left\lfloor \frac{1}{t} (u \cdot c_k + \omega) \right\rfloor$. For the smallest parameter ω, a feasible β-flow in network N_ω corresponds to a feasible flow that minimizes expression (1). Consequently, for minimum parameter ω, a feasible β-flow in network N_ω defines an optimal solution to the MDP.

Before presenting an algorithm to find the minimum parameter ω, we consider the solution values that can be realized in the MDP. The PCP's workload $\Phi_k(\boldsymbol{\alpha}, d_k^w)$ is computed by the anticipated service time t times the number of treatments in session $k \in \mathcal{K}$ which can vary between zero and $D_k := d_k^w + \sum_{k' \in \mathcal{K}_k^-} d_{k'}^r + d^c$. Thus, the possible solution values to the MDP form the finite set $\Omega = \bigcup_{k \in \mathcal{K}} \Omega_k$ with

$$\Omega_k = \left\{ |t \cdot i - u \cdot c_k| \, \big| \, i \in \{0, 1, \dots, D_k\} \right\}.$$

Using this, Algorithm 1 attached to Appendix A computes the optimal parameter $\omega \in \Omega$ based on the following procedure. For the sake of simplicity, binary search is used to first determine the minimum parameter i of set $\{0, 1, \ldots, \max_{k \in \mathcal{K}} D_k\}$ for which a feasible β-flow exists in network $N_{\overline{\omega}}$ with $\overline{\omega} = i \cdot t$. We note that the gap between two consecutive values in set Ω_k, $k \in \mathcal{K}$ is t (if the elements of set Ω_k were ordered by size). Consequently, from the first step, we obtain an interval $(\overline{\omega} - t, \overline{\omega}]$ that contains the optimal parameter ω. In the second step, set Ω is searched for parameters that are within this interval (and smaller than $\overline{\omega}$), i.e., set $(\overline{\omega} - t, \overline{\omega}) \cap \Omega$ is searched. We note that such parameters may exist as the optimal workload $u \cdot c_k$ need not be a multiple of the anticipated service time t. If there are such parameters for which additionally feasible flows in the corresponding networks exist, the minimum parameter found so far is updated. We note that a feasible β-flow can be computed by, for example, the Minimum Mean Cycle Canceling algorithm in polynomial time [35]. Finally, Algorithm 1 returns the minimum parameter $\omega \in \Omega$ and a β-flow that defines an optimal solution to the MDP as shown in the following theorem.

Theorem 1. A mask determined by a β-flow obtained by Algorithm 1 is of minimum cost.

Proof. Let $\omega \in \Omega$ be the parameter and f be the β-flow in network N_ω computed by Algorithm 1. According to Lemma 1, let $\boldsymbol{\alpha}$ and μ be the resulting $(d^c, \boldsymbol{d}^r)$-assignment and mask, respectively. Assume there exists a mask μ^* with less cost, i.e., $c(\mu^*) < c(\mu) = \omega$. There exists a $(d^c, \boldsymbol{d}^r)$-assignment $\boldsymbol{\alpha}^* \in \mathcal{A}^{\mu^*}$ that minimizes the cost of mask μ^*. Based on assignment $\boldsymbol{\alpha}^*$, we can construct a feasible β-flow f^* in network N. We note that each assignment determines a unique flow in network N. Accordingly, there exists a parameter $\omega^* < \omega$ such that f^* is a feasible β-flow in network N_{ω^*}. This contradicts to the correctness of Algorithm 1. $\qquad \square$

We note that the flow obtained by Algorithm 1 is not unique, as for minimum parameter $\omega \in \Omega$ some feasible β-flow in network N_ω is determined. We recall that, for minimum parameter ω, every feasible β-flow in network N_ω defines an optimal solution to the MDP. Using this, we integrate a second optimization stage into our network flow model that takes into account the following. Regular patients strive for an appointment. If they are offered an appointment within their willingness to wait, not only their request is satisfied but also demand is beneficially controlled for the PCP. Considering this win-win situation, we aim at minimizing the unsuccessful appointment requests, or in other words, the number of regular patients who become walk-ins. Regular patients who become walk-ins have not been assigned by a $(d^c, \boldsymbol{d}^r)$-assignment $\boldsymbol{\alpha} = (\alpha^c, \boldsymbol{\alpha}^r)$. In total, that is $d^r_w(\boldsymbol{\alpha}^r) := \sum_{k \in \mathcal{K}} d^r_k - \sum_{k' \in \mathcal{K}^+_k} \alpha^r_k(k')$ regular patients. As assignments are restricted by masks, the number of regular patients who become walk-ins is influenced by the design of a mask. Addressing this in our network flow model, we aim at finding a β-flow in network N_ω for minimum parameter ω with minimum flow value on arcs $(\sigma^r_k, \sigma^w_k) \in A$, $k \in \mathcal{K}$. We can easily implement this into our model by assigning arbitrary positive cost to arcs $(\sigma^r_k, \sigma^w_k) \in A$, $k \in \mathcal{K}$. Overall, we obtain a minimum cost flow model that we integrate into Algorithm 1 by determining a minimum cost β-flow instead of an arbitrary feasible β-flow in the respective network. We refer to the model and procedure presented in this section as *Det-F*. We conclude this section with the following corollary.

Corollary 1. Det-F is a modeling for the MDP.

4.2 MDP in a robust setting

So far, we considered the MDP in a deterministic setting based on the assumption that the entire demand data is given. However, as regular patients contact their PCP when they suffer from acute illnesses, their demand is subject to uncertainty. Naturally, the walk-in demand is also subject to uncertainty. Only the chronic demand is regulated by recurring appointments scheduled in advance. For an effective appointment scheduling system, a mask that is robust against demand uncertainties is essential, i.e., a mask whose use achieves a balanced utilization of the PCP's capacity for all potential demands. Following the core idea of robust optimization, we aim at a version of the MDP whose solution is immune to variation in demand data. To address this issue, we model the uncertainty in regular and walk-in demand by a finite set of scenarios Λ. In each of these scenarios $\lambda \in \Lambda$, the regular and walk-in demands are specified by parameters $\boldsymbol{d}_\lambda^r \in \mathbb{Z}_{\geq 0}^{\mathcal{K}}$ and $\boldsymbol{d}_\lambda^w \in \mathbb{Z}_{\geq 0}^{\mathcal{K}}$, respectively. However, we assume that the variations in demand are limited due to reasons such as a fixed panel of patients. We require the total weekly regular and walk-in demand to be equal for all scenarios, i.e., $\sum_{k \in \mathcal{K}} d_{\lambda,k}^r = D^r$ and $\sum_{k \in \mathcal{K}} d_{\lambda,k}^w = D^w$ for all $\lambda \in \Lambda$ for given parameters $D^r, D^w \in \mathbb{Z}_{\geq 0}$. We note that the chronic demand is still specified by parameter d^c. Given this new setting, we define a mask that is robust to uncertainties in demand.

Definition 6 (Robust Mask). A mask is called *robust* if there exists a compatible $(d^c, \boldsymbol{d}_\lambda^r)$-assignment for each scenario $\lambda \in \Lambda$. The set of all $(d^c, \boldsymbol{d}_\lambda^r)$-assignments that are compatible with mask μ is denoted by $\mathcal{A}_\lambda^\mu$ for every scenario $\lambda \in \Lambda$.

We note that the robustness of a mask is independent of the walk-in demand $\boldsymbol{d}_\lambda^w$, $\lambda \in \Lambda$. Furthermore, we note that the PCP's utilization u and the resulting optimal workload $u \cdot c_k$ in session $k \in \mathcal{K}$ is independent of the scenario considered, as we assume that the total demand is equal in all scenarios. In contrast, the PCP's workload $\Phi_k(\boldsymbol{\alpha}, d_{\lambda,k}^w)$ in session $k \in \mathcal{K}$ depends on a $(d^c, \boldsymbol{d}_\lambda^r)$-assignment $\boldsymbol{\alpha}$ and on walk-in demand $d_{\lambda,k}^w$ and thus on scenario $\lambda \in \Lambda$.

Considering the set of scenarios, we evaluate masks according to the achievable workload balance in the worst-case scenario as formalized in the following definition.

Definition 7. Let the PCP's capacity $\boldsymbol{c} \in \mathbb{Z}_{\geq 0}^{\mathcal{K}}$, demand $d^c \in \mathbb{Z}_{\geq 0}$, and demands $\boldsymbol{d}_\lambda^r, \boldsymbol{d}_\lambda^w \in \mathbb{Z}_{\geq 0}^{\mathcal{K}}$ for all scenarios $\lambda \in \Lambda$ be given. The *cost* of a robust mask μ is defined by the worst-case maximum deviation of the actual from the optimal workload among all sessions of all scenarios, i.e.,

$$c(\mu) = \max_{\lambda \in \Lambda} \min_{\boldsymbol{\alpha} \in \mathcal{A}_\lambda^\mu} \max_{k \in \mathcal{K}} \left| \Phi_k(\boldsymbol{\alpha}, d_{\lambda,k}^w) - u \cdot c_k \right|.$$

Using this, we define a robust version of the MDP as follows.

Definition 8 (rMDP). Let $\boldsymbol{c} \in \mathbb{Z}_{\geq 0}^{\mathcal{K}}$ be the PCP's capacity, $d^c \in \mathbb{Z}_{\geq 0}$ be the chronic demand, and $\boldsymbol{d}_\lambda^r, \boldsymbol{d}_\lambda^w \in \mathbb{Z}_{\geq 0}^{\mathcal{K}}$ be the regular and walk-in demand for all scenarios $\lambda \in \Lambda$, respectively. The *robust mask design problem* aims at a robust mask of minimum cost.

In the next step, we model the rMDP by a network flow and design model in which a so-called robust flow under consistent flow constraints is sought [11]. More precisely, flows are sought for every scenario that satisfy equal flow values on specified arcs. For this purpose, we consider network N as defined in Section 4.1 and adapt the balances to

the set of scenarios. We obtain new balances $\beta^\lambda : V \to \mathbb{Z}$ with $\sum_{v \in V} \beta^\lambda(v) = 0$ for all scenarios $\lambda \in \Lambda$, denoted by $\boldsymbol{\beta} = (\beta^{\lambda_1}, \ldots, \beta^{\lambda_{|\Lambda|}})$, that are defined for all vertices $v \in V$ as follows

$$\beta^\lambda(v) = \begin{cases} d^r_{\lambda,k} & \text{if } v = \sigma^r_k, \ k \in \mathcal{K}, \\ d^w_{\lambda,k} & \text{if } v = \sigma^w_k, \ k \in \mathcal{K}, \\ d^c & \text{if } v = \sigma^c, \\ -\left(d^c + \sum_{k \in \mathcal{K}} \left(d^r_{\lambda,k} + d^w_{\lambda,k} \right) \right) & \text{if } v = \tau, \\ 0 & \text{otherwise.} \end{cases}$$

Furthermore, we introduce two arc sets $A^c_{\text{fix}} := \{(\sigma^c, v^1_k) \mid k \in \mathcal{K}\}$ and $A^r_{\text{fix}} := \{a^1_k \mid k \in \mathcal{K}\}$ and refer to their arcs as *fixed arcs*. Overall, we obtain the adapted network $N^\Lambda = (G, \overline{\psi}, \boldsymbol{\beta})$.

In network N^Λ, a feasible *robust $\boldsymbol{\beta}$-flow* $\boldsymbol{f} = (f^1, \ldots, f^{|\Lambda|})$ is defined by feasible integral β^λ-flows $f^\lambda : A \to \mathbb{Z}_{\geq 0}$ for all scenarios $\lambda \in \Lambda$ that satisfy the following equal flow property

$$(F) \quad f^\lambda(a) = f^{\lambda'}(a) \text{ for all } a \in A^c_{\text{fix}} \cup A^r_{\text{fix}}, \ \lambda, \lambda' \in \Lambda.$$

A robust $\boldsymbol{\beta}$-flow in network N^Λ corresponds to a solution to the rMDP as shown in the following lemma.

Lemma 2. Let $\boldsymbol{f} = (f^1, \ldots, f^{|\Lambda|})$ be a robust $\boldsymbol{\beta}$-flow. Flow $\boldsymbol{f}$ defines

(1) $(d^c, \boldsymbol{d}^r_\lambda)$-assignments $\boldsymbol{\alpha}_\lambda = (\alpha^c, \boldsymbol{\alpha}^r_\lambda)$ with $\alpha^c(k) = f^\lambda((\sigma^c, v^1_k))$ and $\alpha^r_{\lambda,k}(k') = f^\lambda((\sigma^r_k, v^1_{k'}))$ for $\lambda \in \Lambda$, $k \in \mathcal{K}$ and $k' \in \mathcal{K}^+_k$ and

(2) a robust mask $\mu : \mathcal{S} \to \{c, r, w\}, s = (k, q_k) \mapsto \mu(s)$ with

$$\mu(s) = \begin{cases} c & \text{if } q_k \in \{1, \ldots, f^\lambda((\sigma^c, v^1_k))\}, \\ r & \text{if } q_k \in \{f^\lambda((\sigma^c, v^1_k)) + 1, \ldots, f^\lambda(a^1_k)\}, \\ w & \text{otherwise,} \end{cases}$$

for one arbitrary $\lambda \in \Lambda$.

Proof. Analogous to the proof of Lemma 1. $\qquad\square$

We note that the PCP's workload in session $k \in \mathcal{K}$ of scenario $\lambda \in \Lambda$ is given by the respective flow value on treatment arc $a^2_k \in A$, i.e., $\Phi_k(\boldsymbol{\alpha}_\lambda, d^w_{\lambda,k}) = t \cdot f^\lambda(a^2_k)$. Thus, to obtain an optimal solution to the rMDP, we aim at a feasible robust $\boldsymbol{\beta}$-flow $\boldsymbol{f} = (f^1, \ldots, f^{|\Lambda|})$ in network N^Λ that minimizes the following expression

$$\max_{\lambda \in \Lambda} \max_{k \in \mathcal{K}} |t \cdot f^\lambda(a^2_k) - u \cdot c_k|.$$

We recall that $u \cdot c_k$ is still the optimal workload in session $k \in \mathcal{K}$ as the total demand is equal in every scenario. Consequently, the possible solution values to the rMDP are equal to the possible solution values to the MDP contained in set Ω. Analogous to Algorithm 1, we use a procedure to find the minimum parameter $\omega \in \Omega$ for which a feasible robust $\boldsymbol{\beta}$-flow $\boldsymbol{f}$ in network $N^\Lambda_\omega = (G, \overline{\psi}, \underline{\psi}_\omega, \overline{\psi}_\omega, \boldsymbol{\beta})$ exists to determine a solution to the rMDP.

As there does not exist a polynomial-time algorithm to compute a feasible robust flow on acyclic digraphs [11], we determine a feasible robust flow by means of a compact IP. Let $f_a^\lambda \in \mathbb{Z}_{\geq 0}$ be the variables that model the flow on arc $a \in A$ in scenario $\lambda \in \Lambda$. The IP can be formulated as presented in (2)–(7).

$$\min \quad 0 \tag{2}$$

$$\text{s.t.} \quad \sum_{a=(v,w)\in A} f_a^\lambda - \sum_{a=(w,v)\in A} f_a^\lambda = \beta^\lambda(v) \qquad \forall \, v \in V, \, \lambda \in \Lambda \tag{3}$$

$$0 \leq f_a^\lambda \leq \psi(a) \qquad \forall \, a \in A, \lambda \in \Lambda \tag{4}$$

$$\underline{\psi}_\omega(a) \leq f_a^\lambda \leq \overline{\psi}_\omega(a) \qquad \forall \, a = a_k^2 \in A, \, \lambda \in \Lambda \tag{5}$$

$$f_a^\lambda = f_a^{\lambda'} \qquad \forall \, a \in A_{\text{fix}}^r \cup A_{\text{fix}}^c, \, \lambda, \lambda' \in \Lambda \tag{6}$$

$$f_a^\lambda \in \mathbb{Z}_{\geq 0} \qquad \forall \, a \in A, \lambda \in \Lambda \tag{7}$$

The flow balance constraints (3) and capacity constraints (4) ensure feasible flows in all scenarios. Capacity constraints (5) guarantee the desired balanced flow on the treatment arcs. The so-called consistent flow constraints (6) enforce the desired equal flow values on fixed arcs. Constraints (7) define the domain of the variables.

Overall, we can determine a robust $\boldsymbol{\beta}$-flow with minimum parameter $\omega \in \Omega$ that defines an optimal solution to the rMDP problem as stated in the following theorem.

Theorem 2. A robust mask determined by a robust $\boldsymbol{\beta}$-flow obtained by the adjusted Algorithm 1 is of minimum cost.

Proof. Analogous to the proof of Theorem 1. $\qquad\qquad\square$

As a result, for minimum parameter ω, every feasible robust $\boldsymbol{\beta}$-flow in network N_ω^Λ defines an optimal solution to the rMDP. Analogous to Section 4.1, we additionally aim at minimizing the unsuccessful treatment requests, i.e., the total number of regular patients who have not been assigned by a $(d^c, \boldsymbol{d}_\lambda^r)$-assignment $\boldsymbol{\alpha}_\lambda = (\alpha^c, \boldsymbol{\alpha}_\lambda^r)$, $\lambda \in \Lambda$. In total, for all scenarios that is $\sum_{\lambda \in \Lambda} \sum_{k \in \mathcal{K}} d_{\lambda,k}^r - \sum_{k' \in \mathcal{K}_k^+} \alpha_{\lambda,k}^r(k')$. For our extended network flow model, this means that we aim at finding a robust $\boldsymbol{\beta}$-flow in network N_ω^Λ for minimum parameter w, where the sum of the flow values on arcs $(\sigma_k^r, \sigma_k^w) \in A$, $k \in \mathcal{K}$ of all scenarios is minimal. We refer to the resulting model and procedure presented in this section as *Rob-F* and conclude with the following corollary.

Corollary 2. Rob-F is a modeling for the rMDP.

5 Robust multimask design problem and its modeling

In the previous section, we have considered the rMDP where the weekly distribution of the regular and walk-in demands are uncertain, but the respective total demand remains the same in every scenario. Naturally, not only the distribution but also the total demand is uncertain and fluctuates. Under such circumstances, there might not exist a robust

mask, or if it does, it may produce poor results with respect to our objective. To address this issue, we neglect the requirement formulated in the previous section for the total regular and the total walk-in demand. Without further restrictions, the regular and walk-in demand are specified by parameters $\boldsymbol{d}_\lambda^r \in \mathbb{Z}_{\geq 0}^{\mathcal{K}}$ and $\boldsymbol{d}_\lambda^w \in \mathbb{Z}_{\geq 0}^{\mathcal{K}}$ for all scenarios $\lambda \in \Lambda$, respectively. In response to the new setting, we extend the rMDP and employ not only a single robust mask but multiple robust masks. We aim at finding robust masks which are feasible for a cluster of scenarios. Using multiple masks and, in particular, switching between them should allow PCPs to flexibly respond to changes in the demand. To facilitate the switch between masks, we require a nested construction as shown in the following definition. We use the notation $[n] := \{1, \ldots, n\}$.

Definition 9. Masks $\mu^1, \ldots, \mu^n$ are called *nested* if

(1) they have the same number of chronic slots in every session $k \in \mathcal{K}$, i.e., $n_{\mu^i}(c, k) = n_{\mu^j}(c, k)$ for all $i, j \in [n]$ and

(2) mask μ^j has at least as many regular slots as mask μ^i for $i < j$ in every session $k \in \mathcal{K}$, i.e., $n_{\mu^i}(r, k) \leq n_{\mu^j}(r, k)$ for $i < j$ with $i, j \in [n]$.

Given this new setting, we define a robust multimask.

Definition 10 (Robust Multimask). A *multimask* $\boldsymbol{\mu} = (\mu^1, \ldots, \mu^n)$ is defined by a tuple of nested masks $\mu^i : \mathcal{S} \to \{c, r, w\}$, $i \in [n]$. It is called *robust* if a $(d^c, \boldsymbol{d}_\lambda^r)$-assignment exists for each scenario $\lambda \in \Lambda$ that is compatible with at least one of the masks of $\boldsymbol{\mu}$. The set of all $(d^c, \boldsymbol{d}_\lambda^r)$-assignments that are compatible with at least one mask of $\boldsymbol{\mu}$ is denoted by $\mathcal{A}_\lambda^{\boldsymbol{\mu}}$, $\lambda \in \Lambda$.

Before evaluating a robust multimask, we note that the PCP's utilization u_λ depends now on the scenario $\lambda \in \Lambda$, i.e., $u_\lambda = \frac{t}{C} \left(d^c + \sum_{k \in \mathcal{K}} (d_{\lambda,k}^r + d_{\lambda,k}^w) \right)$.

Definition 11. Let the PCP's capacity $\boldsymbol{c} \in \mathbb{Z}_{\geq 0}^{\mathcal{K}}$, demand $d^c \in \mathbb{Z}_{\geq 0}$, and demands $\boldsymbol{d}_\lambda^r, \boldsymbol{d}_\lambda^w \in \mathbb{Z}_{\geq 0}^{\mathcal{K}}$ for all scenarios $\lambda \in \Lambda$ be given. The *cost* of a robust multimask $\boldsymbol{\mu}$ is defined as

$$c(\boldsymbol{\mu}) = \max_{\lambda \in \Lambda} \min_{\boldsymbol{\alpha} \in \mathcal{A}_\lambda^{\boldsymbol{\mu}}} \max_{k \in \mathcal{K}} \left| \Phi_k(\boldsymbol{\alpha}, d_{\lambda,k}^w) - u_\lambda \cdot c_k \right|.$$

Finally, we can define the rMMDP.

Definition 12 (rMMDP). Let $\boldsymbol{c} \in \mathbb{Z}_{\geq 0}^{\mathcal{K}}$ be the PCP's capacity, $d^c \in \mathbb{Z}_{\geq 0}$ be the chronic demand, and $\boldsymbol{d}_\lambda^r, \boldsymbol{d}_\lambda^w \in \mathbb{Z}_{\geq 0}^{\mathcal{K}}$ be the regular and walk-in demand for all scenarios $\lambda \in \Lambda$, respectively. The *robust multimask design problem* aims at finding a robust multimask of minimum cost.

In the following, we also model the rMMDP by a network flow and design model. Therefore, let $\pi : \Lambda \to \{\mu^1, \ldots, \mu^n\}$ be a function that allocates one mask to each scenario. In network N^Λ, a feasible *nested robust $\boldsymbol{\beta}$-flow* $\boldsymbol{f} = (f^1, \ldots, f^{|\Lambda|})$ is defined by feasible integral β^λ-flows $f^\lambda : A \to \mathbb{Z}_{\geq 0}$ for all scenarios $\lambda \in \Lambda$ that satisfy the flow properties presented in $(F1) - (F3)$:

$(F1)$ $f^\lambda(a) = f^{\lambda'}(a)$ for all $a \in A_{\text{fix}}^c$ and $\lambda, \lambda' \in \Lambda$,

$(F2)$ $f^\lambda(a) = f^{\lambda'}(a)$ for all $a \in A_{\text{fix}}^r$ and $\lambda, \lambda' \in \Lambda$ with $\pi(\lambda) = \pi(\lambda')$,

$(F3)$ $f^\lambda(a) \leq f^{\lambda'}(a)$ for all $a \in A_{\text{fix}}^r$ and $\lambda, \lambda' \in \Lambda$ where $\lambda \in \pi^{-1}(\mu^i)$, $\lambda' \in \pi^{-1}(\mu^j)$, $i \leq j$.

Flow property $(F1)$ ensures that the flow value on a fixed arc contained in set A_fix^c is equal among all scenarios. Flow property $(F2)$ ensures that the flow value on a fixed arc contained in set A_fix^r is equal for all scenarios which are assigned to the same mask. Flow property $(F3)$ ensures non-decreasing flow values on fixed arcs contained in set A_fix^r among scenarios assigned to different masks. A nested robust $\boldsymbol{\beta}$-flow in network N^Λ corresponds to a solution to the rMMDP as shown in the following lemma.

Lemma 3. Let $\boldsymbol{f} = (f^1, \ldots, f^{|\Lambda|})$ be a nested robust $\boldsymbol{\beta}$-flow. Flow $\boldsymbol{f}$ defines

(1) $(d^c, \boldsymbol{d}_\lambda^r)$-assignments $\boldsymbol{\alpha}_\lambda = (\alpha^c, \boldsymbol{\alpha}_\lambda^r)$ with $\alpha^c(k) = f^\lambda((\sigma^c, v_k^1))$ and $\alpha_{\lambda,k}^r(k') = f^\lambda((\sigma_k^r, v_{k'}^1))$ for $\lambda \in \Lambda$, $k \in \mathcal{K}$ and $k' \in \mathcal{K}_k^+$ and

(2) a multimask $\boldsymbol{\mu} = (\mu^1, \ldots, \mu^n)$ with $\mu^i : \mathcal{S} \to \{c, r, w\}, s = (k, q_k) \mapsto \mu^i(s)$, $i \in [n]$ for $\lambda \in \pi^{-1}(\mu^i)$ as follows

$$\mu^i(s) = \begin{cases} c & \text{if } q_k \in \{1, \ldots, f^\lambda((\sigma^c, v_k^1))\}, \\ r & \text{if } q_k \in \{f^\lambda((\sigma^c, v_k^1)) + 1, \ldots, f^\lambda(a_k^1)\}, \\ w & \text{otherwise.} \end{cases}$$

Proof. The proof can be done analogously to the proof of Lemma 1. $\qquad \square$

To obtain an optimal solution to the rMMDP, we aim at a feasible nested robust $\boldsymbol{\beta}$-flow $\boldsymbol{f} = (f^1, \ldots, f^{|\Lambda|})$ in network N^Λ that minimizes the following expression

$$\max_{\lambda \in \Lambda} \max_{k \in \mathcal{K}} |t \cdot f^\lambda(a_k^2) - u_\lambda \cdot c_k|.$$

In contrast to the rMDP, the solution space of the rMMDP differs among the scenarios as the PCP's utilization depends on the scenario considered. The possible solution values form the finite set $\Omega^\Lambda = \bigcup_{\lambda \in \Lambda, k \in \mathcal{K}} \Omega_{\lambda,k}$ with

$$\Omega_{\lambda,k} = \left\{ |t \cdot i - u_\lambda \cdot c_k| \,\middle|\, i \in \{0, 1, \ldots, D_{\lambda,k}\} \right\},$$

where $D_{\lambda,k} = d_{\lambda,k}^w + \sum_{k' \in \mathcal{K}_k^-} d_{\lambda,k'}^r + d^c$. Analogous to the previous section, we use an adjusted version of Algorithm 1 to find the minimum parameter $\omega \in \Omega^\Lambda$ for which a feasible nested robust $\boldsymbol{\beta}$-flow $\boldsymbol{f}$ exists in network N_ω^Λ to determine a solution to the rMMDP. We determine a feasible nested robust flow using a compact IP formulation. Let $f_a^\lambda \in \mathbb{Z}_{\geq 0}$ be the variables that model the flow on arc $a \in A$ in scenario $\lambda \in \Lambda$. Let $m_k^i \in \mathbb{Z}_{\geq 0}$, $i \in [n]$ be auxiliary variables that indicate the amount of flow on arcs $a_k^i \in A$. Further, let $y_\lambda^i \in \{0, 1\}$ be binary variables that determine whether a mask μ^i, $i \in [n]$ is allocated to scenario $\lambda \in \Lambda$ ($y_\lambda^i = 1$) or not ($y_\lambda^i = 0$), corresponding to function π. The

IP can be formulated as presented in (8)–(19).

$$\min \ 0 \tag{8}$$

$$\text{s.t.} \quad \sum_{a=(v,w)\in A} f_a^\lambda - \sum_{a=(w,v)\in A} f_a^\lambda = \beta^\lambda(v) \qquad \forall \ v \in V, \ \lambda \in \Lambda \tag{9}$$

$$0 \le f_a^\lambda \le \psi(a) \qquad \forall \ a \in A, \ \lambda \in \Lambda \tag{10}$$

$$\underline{\psi}_\omega(a) \le f_a^\lambda \le \overline{\psi}_\omega(a) \qquad \forall \ a = a_k^2 \in A, \ \lambda \in \Lambda \tag{11}$$

$$f_a^\lambda = f_a^{\lambda'} \qquad \forall \ a \in A_c^{\text{fix}}, \ \lambda, \lambda' \in \Lambda \tag{12}$$

$$\sum_{i=1}^n y_\lambda^i = 1 \qquad \forall \ \lambda \in \Lambda \tag{13}$$

$$f_{a_k^1}^\lambda \le m_k^i + n_k(1 - y_\lambda^i) \qquad \forall \ i \in [n], \ k \in \mathcal{K}, \ \lambda \in \Lambda \tag{14}$$

$$f_{a_k^1}^\lambda \ge m_k^i - n_k(1 - y_\lambda^i) \qquad \forall \ i \in [n], \ k \in \mathcal{K}, \ \lambda \in \Lambda \tag{15}$$

$$m_k^i \le m_k^{i+1} \qquad \forall \ i \in [n-1], \ k \in \mathcal{K} \tag{16}$$

$$f_a^\lambda \in \mathbb{Z}_{\ge 0} \qquad \forall \ a \in A, \ \lambda \in \Lambda \tag{17}$$

$$m_k^i \in \mathbb{Z}_{\ge 0} \qquad \forall \ i \in [n], \ k \in \mathcal{K} \tag{18}$$

$$y_\lambda^i \in \{0,1\} \qquad \forall \ i \in [n], \ \lambda \in \Lambda \tag{19}$$

The flow balance constraints (9) and capacity constraints (10) ensure feasible flows in all scenarios. Capacity constraints (11) guarantee the desired balanced flow on the treatment arcs. Constraints (12) enforce the equal flow values on arcs $a \in A_c^{\text{fix}}$ among all scenarios as required in flow property $(F1)$. Constraints (13) model that one mask is assigned to each scenario which corresponds to function π. Constraints (14) and (15) enforce the equal flow values on arcs $a \in A_r^{\text{fix}}$ (in amount of m_k^i) for two scenarios $\lambda, \lambda' \in \Lambda$ if the scenarios are assigned to the same mask, i.e., $\mu^i = \pi(\lambda) = \pi(\lambda')$, $i \in [n]$ ($y_\lambda^i = y_{\lambda'}^i = 1$), as required in flow property $(F2)$. Otherwise, they function only as upper and lower bounds on the flows. The combination of constraints (14)–(16) enforce the non-decreasing flow values on arcs $a \in A_r^{\text{fix}}$ for two scenarios $\lambda, \lambda' \in \Lambda$ if the scenarios are assigned to different masks μ^i, μ^j with $i \le j$, i.e., $\mu^i = \pi(\lambda)$ and $\mu^j = \pi(\lambda')$ ($y_\lambda^i = y_{\lambda'}^j = 1$), as required in flow property $(F3)$. Finally, constraints (17)–(19) define the domain of the variables.

Overall, we can determine a nested robust $\boldsymbol{\beta}$-flow in network N_ω^Λ with minimum parameter $\omega \in \Omega^\Lambda$ that defines an optimal solution to the rMMDP problem as shown in the following theorem.

Theorem 3. A robust multimask determined by a nested robust $\boldsymbol{\beta}$-flow obtained by the adjusted Algorithm 1 is of minimum cost.

Proof. Analogous to the proof of Theorem 1. □

Analogous to Section 4.1, if we aim at finding a nested robust $\boldsymbol{\beta}$-flow in network N_ω^Λ for minimum parameter $w \in \Omega^\Lambda$ with minimum flow value on arcs $(\sigma_k^r, \sigma_k^w) \in A$, $k \in \mathcal{K}$, we can additionally minimize the number of regular patients who become walk-ins. We refer to the extended model and procedure presented in this section as *RobMulti-F*. Finally, we obtain the following corollary.

Corollary 3. RobMulti-F is a modeling for the rMMDP.

6 Case study

In this section, we present a case study conducted to demonstrate the potential of the mask-based appointment scheduling systems obtained by solving MDP, rMDP, and rMMDP. In Section 6.1, we present the experimental environment. In Section 6.2, we present the setting of the implementation and computation. In Section 6.3, we discuss the results of the optimization models. In Section 6.4, we evaluate the mask-based appointment scheduling systems and compare them with some appointment scheduling systems from the literature using agent-based simulation.

6.1 Experimental environment

In this section, we present the experimental environment for the case study. This includes the physician-patients setting, the simulation model and its input data, and the appointment scheduling systems. In addition, this includes the instance generation and input parameter for the optimization models.

6.1.1 Physician-patients setting

In primary health care, the physician-to-patient ratio is commonly used to measure medical care. Following the German Federal Joint Committee's (GFJC) guideline [16], we set the ratio of one PCP per 1607 patients as a benchmark for analyzing the appointment scheduling systems in this study. The GFJC defines an excess of 10% in the ratio as oversupply, i.e., one PCP per 1448 patients. An undersupply is defined by a 25% shortfall in the ratio, i.e., one PCP per 2011 patients. Representing these three scenarios, we analyze the performance of the appointment scheduling systems for populations of 1400, 1600, and 2000 patients. According to a study of the German Robert Koch Institute [28], 43% of female and 38% of male patients are chronically ill. As our study is gender neutral, we consider 40% of all patients to be suffering from chronic illnesses. Due to the worldwide aging population at the highest risk of chronic conditions, an increase in the number of chronically ill patients is expected. Thus, we additionally analyze a chronic proportion of 45%. Over the past ten years, surveys conducted by The National Association of Statutory Health Insurance Physicians [42] have revealed that on average 18.8% of the patients holding health insurance are walk-ins that forgo scheduling an appointment with their PCPs. To cover this and slight deviations, we analyze a walk-in rate of 15%, 18%, and 20%. In total, we obtain 18 different configurations for the patient population considered in this case study, as summarized in Table 1.

Config. ID	# patients	chronic. ill (%)	walk-in rate (%)
1	1400	40	15
2	1400	40	18
3	1400	40	20
4	1400	45	15
5	1400	45	18
6	1400	45	20
7	1600	40	15
8	1600	40	18
9	1600	40	20
10	1600	45	15
11	1600	45	18
12	1600	45	20
13	2000	40	15
14	2000	40	18
15	2000	40	20
16	2000	45	15
17	2000	45	18
18	2000	45	20

Table 1: Patient configurations

Based on a survey regarding the practice's opening hours conducted by The National Association of Statutory Health Insurance Funds [20], we determine the PCP's opening hours as follows. We decide the PCP to operate in a four-hour morning session from Monday to Friday and in a two-and-a-half-hour afternoon session on Mondays, Tuesdays, and Thursdays. This results in a time span $o_{(i,0)} = 240$ for $i \in \{0, \dots, 4\}$ and $o_{(i,1)} = 150$ for $i \in \{0, 1, 3\}$. The first hour after each session is used as buffer time, i.e., $b_k = 60$ for all $k \in \mathcal{K}$. Accordingly, overtime is caused if the PCP works beyond the capacity $c_{(i,0)} = 300$ for $i \in \{0, \dots, 4\}$ and $c_{(i,1)} = 210$ for $i \in \{0, 1, 3\}$.

6.1.2 Simulation model SiM-Care and modifications

To generate instances and to analyze the appointment scheduling systems designed in this study, we use the agent-based simulation tool 'SiM-Care' (Simulation Model for Primary Care) [15]. SiM-Care simulates the dynamics of primary health care systems and aims at supporting decision-makers in their planning, analysis, and adaption. For this purpose, it models PCPs, patients, and their interaction on an individual level. Tracking the interactions allows identifying the interdependencies between different subproblems, evaluating new planning approaches, and quantifying the effects of interventions based on multiple performance measurements. SiM-Care enables in particular the comparison and assessment of appointment scheduling systems in terms of, for example, patients' waiting times, patients' access times, or the PCPs' utilization. For the sake of validity, SiM-Care uses real-world data to the extent available. For example, the distribution of illnesses and their characteristics are estimated on the basis of publications of health insurances and federal government agencies. All unavailable data was either empirically collected in

a primary care practice, for instance the patients' service times, or where this was not possible, it was inferred.

To simulate the needs of our primary health care setting, we make the following changes to SiM-Care. First, in the current modeling, PCPs may reject patients due to capacity overloads. Rejected patients then seek care at other PCPs. As we only consider one PCP in our study, we integrate an emergency practice to SiM-Care. Accordingly, if patients are rejected by the PCP in our setting, they seek immediate care at a physician in the emergency practice. Second, in the current modeling, patients always try to make a feasible appointment first. If they do not succeed, they seek immediate care as walk-ins. However, there always exist walk-ins who have not previously attempted to make an appointment. For this reason, we integrate that a given percentage of the patients forgo making an appointment and instead seek immediate care as walk-in. At this point, we note that patients who successfully make an appointment actually attend it, i.e., there are no no-shows modeled. Furthermore, we note that, in contrast to our optimization models, in SiM-Care, the patients' willingness to wait for an appointment is individual for each patient, as it depends on factors such as the illness, the age, and the condition of the patients. Third, we assume that walk-ins are subject to the same service time distribution as patients with appointments. We note that the service times are sampled from a maximum likelihood fitted log-normal distribution based on empirical service times. The result is a mean service time of 7.8 minutes.

Before addressing the input parameters for SiM-Care in the next section, we note that SiM-Care is a complex simulation model, much more complex than our optimization models. We have chosen SiM-Care on an operational decision level to prove that the optimization models developed on a tactical decision level can withstand complex systems.

6.1.3 Input parameters for SiM-Care

Comis et al. [15] present a case study for a primary health care system in Germany to showcase SiM-Care and its validation through expert input and empirical data. Specifically, they create a baseline scenario representing a real-world primary health care system. In this study, we conduct a case study based on this baseline scenario. In particular, we assume the same age classes and age-class-illness distributions. In the following, we detail the input parameter choices that are different from this baseline scenario.

First, we model a time period of one year (52 weeks) preceded by a warm-up period of also one year. Second, we consider randomly generated locations of the patients and physicians as performance indicators such as travel times are not important in our case study. Third, the modeled PCP and their opening hours as well as the modeled patients are as described in Section 6.1.1. Fourth, we consider the same families of illnesses as in the baseline scenario, consisting of three chronic and four acute illnesses, which is a subset of the 100 ICD-10 codes most frequently reported to the Association of Statutory Health Insurance Physicians Nordrhein [30]. Fifth, we apply the same estimation for the attributes of the families of illnesses as real data is protected by confidentiality and not published. The only difference is that we assume that patients with acute illnesses do not require a follow-up treatment (i.e., the treatment frequency is not applicable). Finally, we present the integrated appointment scheduling, the treatment, and the admission strategy employed by the PCP modeled in SiM-Care. The integrated appointment scheduling strategies are detailed in Section 6.1.4. The treatment strategy is defined as in the baseline
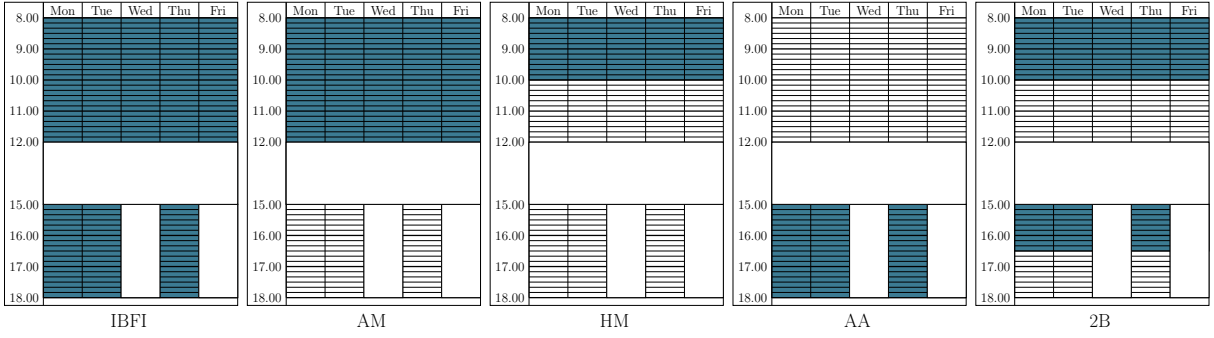
Figure 4: Non-mask-based systems from the literature with slots ▬ reserved for appointments and slots ▭ withheld for walk-ins

scenario [15]. The strategy includes the order of treatments on a priority-first-come-first-served basis: Patients with appointment are prioritized over walk-ins and within their respective groups, patients are served in order of their arrivals, i.e., first come, first served. In addition, the treatment strategy includes the PCP's consultation speed, that is, the PCP adjusts the service times whenever more than three patients await treatment. The admission strategy is defined as follows. Patients with an appointment are admitted as long as they arrive before the end of the buffer time. Like in studies [32, 45], walk-ins are admitted up to a certain utilization threshold. Therefore, PCPs predict their remaining workload by multiplying the average service time of 7.8 minutes with the number of currently waiting patients and upcoming scheduled appointments. If this estimated workload is lower than the remaining duration of the current session including buffer time, walk-ins are admitted, otherwise rejected.

6.1.4 Appointment scheduling systems

In this section, we present the PCP's appointment scheduling strategies, or in other words, the appointment scheduling systems that we implement in SiM-Care for this study. Before presenting the considered appointment scheduling systems, we note that they are based on slot systems. To that end, the opening hours of each session are divided into slots of 10 minutes length. Theoretically, each slot can accommodate one appointment. However, the appointment scheduling systems determine which slots are allowed to accommodate an appointment. In SiM-Care, appointments are offered to patients on a first-come-first-serve basis. Consequently, every patient is offered the earliest feasible appointment at the time of inquiry. If no feasible appointment is available, the patient decides to forgo an appointment and seek immediate care as walk-in. An offered appointment is feasible for a patient if it matches with the patient's availabilities and if it is within the patient's willingness to wait. In the following, we list the implemented appointment scheduling systems. We refer to Figure 4 which visualizes the five appointment scheduling systems derived from the literature.

Individual-block/Fixed-interval (IBFI)   Like Comis et al. [15], we consider the IBFI appointment scheduling system. IBFI allows all slots of each session to accommodate an appointment [12, 34]. Thus, no slots are withheld.

All Morning (AM) and Half Morning (HM)   Like Balasubramanian et al. [6] and Wiesche et al. [54], we consider the AM and the HM appointment scheduling system as benchmarks. AM allows all slots of each morning session to accommodate an appointment. HM allows the first half of the slots of each morning session to accommodate an appointment. In both appointment scheduling systems, the slots of every afternoon session are withheld for the treatment of walk-ins.

All Afternoon (AA)   Like Balasubramanian et al. [6], we consider the AA appointment scheduling system as a benchmark. AA allows all slots of each afternoon session to accommodate an appointment. The slots of every morning session are withheld for the treatment of walk-ins.

2-Block (2B)   We consider the 2B appointment scheduling system introduced by Balasubramanian et al. [6]. 2B allows the slots of the first half of each session to accommodate an appointment. The slots of the second half of each session are withheld for the treatment of walk-ins.

Masked-Based (M) and Robust-Mask-Based (RM)   We consider the M and the RM appointment scheduling systems that are based on a mask and a robust mask obtained by solving MDP and rMDP, respectively. M and RM allow in each session the chronic and regular slots to accommodate an appointment for one chronic or regular patient, respectively. The walk-in slots of each session are withheld for the treatment of walk-ins.

Multimask-Based (MM)   We consider the MM appointment scheduling system based on a multimask consisting of three nested masks obtained by solving rMMDP. MM allows in each session the chronic and regular slots to accommodate an appointment for one chronic or regular patient, respectively. In addition to the standard scheduling process for chronic patients, the scheduling process for regular patients based on the multimask is as follows. Every regular patient is offered the earliest feasible appointment of the first mask at the time of inquiry. If the earliest feasible appointment is not within the patient's willingness to wait, the patient is offered the earliest feasible appointment of the second and if necessary of the third mask. The walk-in slots of each session are withheld for the treatment of walk-ins.

Before we conclude this section, we note that we refer to AM, HM, and AA as benchmark systems. Furthermore, we refer to IBFI, AM, HM, AA, 2B as non-mask-based systems and to M, RM, and MM as mask-based systems. We conclude this section by noting that the non-mask-based systems do not distinguish between slots reserved explicitly for regular or chronic patients.

6.1.5 Instance generation for (robust) mask and robust multimask design problem

For the instances of MDP, rMDP, and rMMDP, demand data is crucial. In the absence of accessible empirical data on visits to primary care practices, we have to rely on simulation to obtain rough estimates. Based on a selected patient configuration presented in Section 6.1.1, we use SiM-Care [15] to simulate the number of visits to a primary care

practice by regular and chronic patients as well as walk-ins over a one-year time horizon. We obtain the demand of 52 weeks and classify it into regular, chronic, and walk-in demand. We prepare this demand data as input to our optimization problems as explained in the following.

For the MDP, we average the demand of the 52 weeks and obtain the session-specific regular and walk-in demands $\boldsymbol{d}^r$ and $\boldsymbol{d}^w$ and the weekly chronic demand d^c. For the rMDP and the rMMDP, we require different scenarios, where each scenario consists of one week's demand. For the input of both problems, we use the scenario set $\Lambda^{52} = \{\lambda_1, \dots, \lambda_{52}\}$ that is obtained by considering the demand from each of the 52 weeks of the year as individual scenarios. As shown in the next section, the model RobMulti-F cannot optimally solve all instances to the rMMDP within the given time limit. In addition, we note that there is a risk of overfitting for the robust model Rob-F if the scenario set is too large due to the strict equal flow property (F). The same holds true for RobMulti-F due to the strict equal flow properties $(F1)$ and $(F2)$. For this reason, we use a second scenario set Λ^{13} as input for the rMDP and the rMMDP. Scenario set $\Lambda^{13} = \{\lambda_1, \dots, \lambda_{13}\}$ is constructed by aggregating the demand of each four consecutive weeks of the 52 weeks to create 13 different scenarios. For the two scenario sets Λ^{52} and Λ^{13}, we perform the following additional processing to obtain valid inputs to the optimization problems. For the rMDP, we standardize the regular and walk-in demand so that the total regular and walk-in demand is equal in all scenarios, i.e., $\sum_{k \in \mathcal{K}} d^r_{\lambda,k} = D^r$ and $\sum_{k \in \mathcal{K}} d^w_{\lambda,k} = D^w$ for all $\lambda \in \Lambda^{52}$, $\lambda \in \Lambda^{13}$. Furthermore, we standardize the chronic demand as in rMDP the chronic demand is specified by only one parameter d^c. For the rMMDP, we only need to standardize the chronic demand.

Since SiM-Care relies on stochastic values, our case study includes ten independent runs. Therefore, we perform the demand generation and processing described above ten times for each patient configuration. Given the ten runs for the 18 different patient configurations, we obtain a total of 180 instances for Det-F and, due to the two different scenario sets considered, 360 instances for Rob-F and RobMulti-F. Besides the demand data, the optimization problems MDP, rMDP, and rMMDP require the following input parameters. For each of the three optimization problems, we set the uniform anticipated service time t according to the mean service time in SiM-Care, which averages 7.8 minutes. Adjusted to the anticipated service time, we determine ten-minutes slots, i.e., $\ell = 10$. The capacity and buffer time of the PCP is set as described in Section 6.1.1. For the rMMDP, we consider multimasks that consist of three nested masks, i.e., $n = 3$.

6.2 Implementation and computational setting

For our computational study, all computational experiments are performed on a cluster of machines running Ubuntu 20.04.6 with an Intel(R) Core(TM) $i9 - 9900$ CPU @ 3.10 GHz and 32 GB DDR4-Non-ECC main memory. We restrict each individual job to one physical core, 14 GB main memory, and a time of 24 hours. We implement our algorithms based on binary search and IP formulations in Java using OpenJDK 11 [33]. To solve the IP formulations, we use CPLEX 22.1 through the Java API [1]. We restrict the CPLEX optimizer to a one hour time limit and 32 GB memory limit and leave all other CPLEX parameters at their default settings.

We solve the MDP, rMDP, and rMMDP by using the models Det-F, Rob-F, and RobMulti-F, respectively. Each model includes two optimization stages as presented in

Sections [4.1], [4.2], and [5]. In theory, we can solve both stages at once by determining flows of minimum cost instead of feasible flows. In contrast, when solving the models, we consider the stages separately and sequentially to speed up the computations. In the first optimization stage, we aim at finding the minimum parameter $\omega \in \Omega$ (Ω^Λ) for which a feasible flow in network N_ω (N_ω^Λ) exists by binary search. Once the minimum parameter $\omega \in \Omega$ (Ω^Λ) is found, we proceed with the second optimization stage. In the second optimization stage, we aim at finding a minimum cost flow, robust flow, or robust nested flow in network N_ω (N_ω^Λ). We recall that there does not exist a polynomial-time algorithm to determine a robust or a robust nested flow. Therefore and for simplicity's sake, we compute all flows of all models, including the deterministic model, by IPs. While runtime is clearly not a focus of this study, we note the following regarding the solvability. The first optimization stage is performed in a few seconds for most instances and in less than two hours for every instance. Consequently, for all instances an optimal solution to the first stage and thus a feasible solution to the second stage is found. The second optimization stage is solved to optimality (CPLEX default MIP gap tolerance 10^{-4}) for all instances of Det-F and Rob-F within the given time limit of one hour. In contrast, it is solved to optimality for only 100 out of the 180 instances based on scenario set Λ^{52} of RobMulti-F within the given time limit of one hour. For the remaining 80 instances, the best solution found so far is considered. As described in Section [6.1.5], due to non-solvability within the given time limit, we additionally consider instances based on scenario set Λ^{13} as input for the optimization problems Rob-F and RobMulti-F. For scenario set Λ^{13}, all instances of both models are solved to optimality within the given time limit.

6.3 Evaluation of the optimization models and the resulting masks

In this section, we analyze the results of the Det-F, the Rob-F, and the RobMulti-F model. Before we begin, we recall the following. The solution of each model provides us with the following three results. First, we obtain the objective value $\omega \in \mathbb{Z}_{\geq 0}$ for which the respective flow with minimum cost is found in the corresponding network. Second, we obtain the number of the unsuccessful appointment requests ($d_w^r(\cdot)$) by the cost of the flow. Third, we obtain a mask (of cost ω) and thus the number of chronic, regular, and walk-in slots ($\sum_{k \in \mathcal{K}} n_\mu(\cdot, k)$) by the flow itself. For all instances, the results of the three models are summarized in Tables [2–7] in Appendix [B].

We start by considering the objective value ω. For each model, the average objective value of the ten runs are visualized for all patient configurations and both scenario sets in Figure [5]. We note that the results of Det-F are not computed based on the demands of the scenario sets Λ^{52} and Λ^{13}, instead the input is the average annual demand. The double visualization is only for the comparability of the models. For Rob-F and RobMulti-F, the average objective value ω is affected by the choice of the scenario set. We confirm that the results for scenario set Λ^{52} are significantly higher than those for scenario set Λ^{13}. This meets our expectations as the computation of the minimum parameter ω becomes more difficult the more scenarios are considered in the sense that the parameter must be suitable for more scenarios. Accordingly, Det-F achieves the best average objective values since the minimum parameter ω is determined for only a single demand scenario. Considering the fact that the objective value ω corresponds to the cost of an optimal mask, we have to pay on average higher cost of a robust or robust nested mask compared to a non-robust mask, the so-called price of robustness [8]. In addition, RobMulti-F achieves on average better
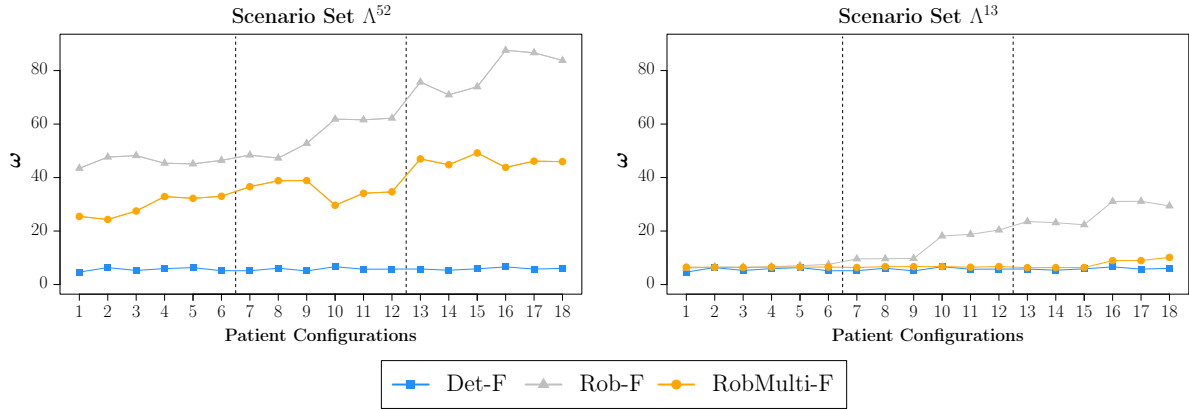
Figure 5: The cost of masks depending on the scenario set, patient configuration, and optimization model
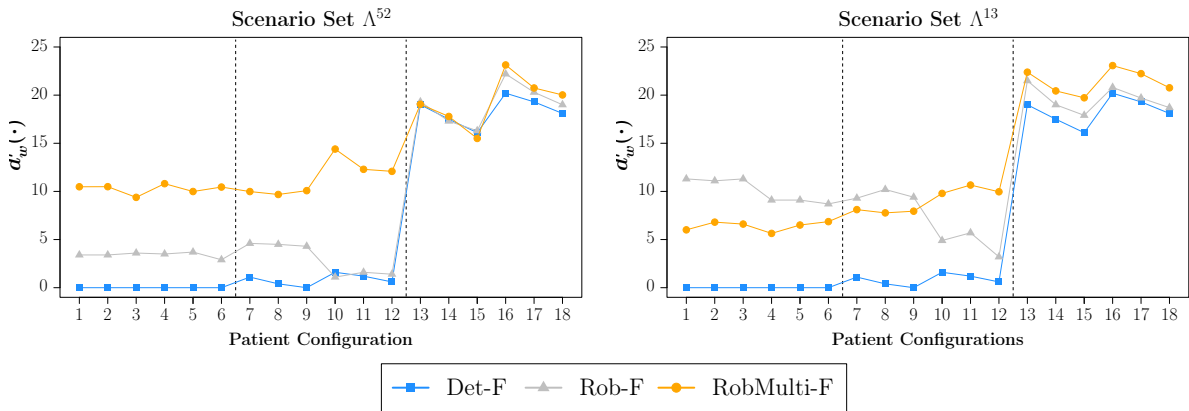
Figure 6: Average number of unsuccessful appointment requests

objective values than Rob-F due to the higher flexibility of a robust nested multimask compared to a robust mask. For scenario set Λ^{52}, RobMulti-F outperforms Rob-F in all patients configurations. For scenario set Λ^{13}, this is mainly observed in the patient configurations $7-18$ that represent increased demand based on population of 1600 and 2000 patients. Furthermore, Rob-F and RobMulti-F have the tendency that the average objective value ω increases (with exceptions) the more patients are considered (patient configurations $1-6$ versus $7-12$ versus $13-18$). Finally, recall that parameter ω, or in other words, the cost of a corresponding mask indicates the deviation of the PCP's actual workload from the optimal workload using the respective model.

In the next step, we consider the total number of unsuccessful treatment requests $(d_w^r(\cdot))$. For each model, we average the total number of unsuccessful appointment requests over the number of scenarios to obtain the average number per scenario. We visualize the average of the ten runs for all patient configurations and both scenario sets in Figure 6. We recall that RobMulti-F is solved to feasibility (i.e., the minimum parameter ω is found) but not to optimality for all instances based on scenario set Λ^{52}. For these cases, the minimum total number of unsuccessful treatment requests found so far is considered. Furthermore, we recall that the results of Det-F are not based on the scenario sets Λ^{52} and Λ^{13}. The input is the average annual demand. Det-F satisfies all appointment requests

26

for patient configurations $1 - 6$ and misses only a maximum average of 1.6 requests for patient configurations $7 - 12$. In contrast, Det-F performs significantly worse for the patient configurations $13 - 18$ based on the population of 2000 patients with average unsuccessful appointment requests between 16.1 and 20.2. For Rob-F and RobMulti-F, the average number of unsuccessful appointment requests is affected by the choice of the scenario set. For patient configurations $1 - 12$, the results of Rob-F are clearly lower than those of RobMulti-F for scenario set Λ^{52} while the opposite is the case for scenario set Λ^{13}. We explain this by the following two reasons. First, as RobMulti-F is not optimally solved for all instances based on scenario set Λ^{52} (unlike set Λ^{13}), only the best results found so far are considered for the total number of unsuccessful treatment requests. Second, the results of the objective values ω of Rob-F are significantly higher for instances based on scenario set Λ^{52} than set Λ^{13}. Consequently, the solutions to Rob-F based on scenario set Λ^{52} allow a higher deviation of the actual from the optimal PCP's workload which in turn provides more flexibility for appointments so that there are fewer unsuccessful appointment requests. Like Det-F, Rob-F and RobMulti-F perform for patient configurations $13 - 18$ significantly worse than for all other configurations. Consistent with the results, we expect that if the total number of patients increases while the PCP's capacity remains the same, the number of unsuccessful appointment requests increases. Counterintuitive are the outliers of Rob-F for patient configurations $10 - 12$. However, if we consider the objective values ω of Rob-F for the same configurations, we see that they are significantly higher than the objective values of configurations $7 - 9$, although in both cases the configurations are based on the same size of the population of patients. This means that the solutions to Rob-F allow a higher deviation of the actual from the optimal PCP's workload for patient configurations $10 - 12$ than for configurations $7 - 9$. Thus, for patient configurations $10 - 12$, the solutions to Rob-F also provide more flexibility for appointments so that there are fewer unsuccessful appointment requests. A second result we expect is that if the walk-in rate increases, the number of patients that request an appointment decreases. Consequently, the number of unsuccessful appointment requests also decreases. In particular, this effect can be observed in the results of Det-F for all patient configurations and in the results of all three models for configurations $13 - 18$. We conclude with the following note. The number of unsuccessful appointment requests provides us with the information that, given an allowed maximum deviation, there is theoretically no assignment of the patient demand that would satisfy every appointment requests.

Finally, we consider the structure of the masks, robust masks, and nested robust masks that result from the optimization models Det-F, Rob-F, and RobMulti-F, respectively. Before discussing the results, we note that there are in total $|\mathcal{S}| = 165$ slots within the PCP's capacity. Furthermore, we note that in all three models, d^c out of the 165 slots are assigned the state 'chronic'. Consequently, the number of available slots for state 'regular' or 'walk-in' is $165 - d^c$. In the following, we only compare the number of regular slots of the masks among all models. We recall that all remaining slots are walk-in slots. For each model, the total number of regular slots is averaged over the ten runs and visualized for all patient configurations and both scenario sets in Figure 7. Furthermore, we recall that the number of available slots for state 'regular' as well as the results of Det-F are independent from the scenario sets.

First of all, we confirm that the number of slots available for state 'regular' decreases if the population of patients and thus the proportion of chronic patients increases. Moreover,
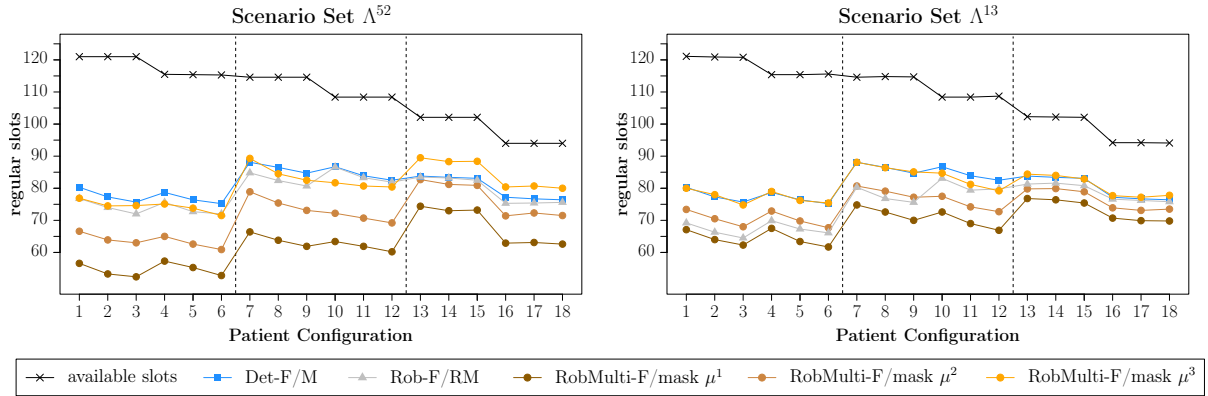
Figure 7: Average number of regular slots of the masks

we note that none of the models assigns all available slots to the state 'regular'. Conversely, in all models there are slots assigned the state 'walk-in'. For Det-F, the average total number of regular slots is at a high level compared to the results of the other models and varies between 75.2 and 88.1, depending on the patient configuration. For Rob-F and RobMulti-F, the total numbers of regular slots are affected by the choice of the scenario set. Before discussing the differences, we confirm for RobMulti-F the resulting nested masks, denoted by μ^1, μ^2, μ^3. Considering Rob-F, we see that the total number of regular slots is significantly higher for the robust mask based on scenario set Λ^{52} than set Λ^{13}. For RobMulti-F based on scenario set Λ^{52}, we note that the total number of regular slots of the third mask is lower than those from Det-F neglecting patient configurations $13-18$. In contrast, for RobMulti-F based on scenario set Λ^{13}, the results almost coincide with those from Det-F. Moreover, we note that the difference of the number of regular slots between the three resulting masks is smaller for RobMulti-F based on scenario set Λ^{13} than on set Λ^{52}. We explain this by the overall fewer and less diverse demand scenarios of set Λ^{13} used for the computation of the solution due to the aggregation of the scenarios. Furthermore, we see that each of the three masks based on scenario set Λ^{13} offers more regular slots than each of the corresponding masks based on set Λ^{52}. All three models have the tendency that the total number of regular slots decreases if the walk-in rate increases as seen in patient configurations $1-3$, $4-6$, $7-9$, $10-12$, $13-15$, and $16-18$.

Before concluding the section, we analyze how often each of the three resulting masks of RobMulti-F is used among all scenarios. Figure 8 visualizes the average frequency over all 10 runs of the assignment of masks μ^1, μ^2, and μ^3 to the scenarios of scenario sets Λ^{52} and Λ^{13} for all patient configurations. In general, we confirm that the average use of the masks μ^1, μ^2, and μ^3 is balanced for all patient configurations, so none of the masks is tailored exclusively for one scenario. Instead, we see that each of the three masks is assigned for a cluster of scenarios as targeted in Section 5. For scenario set Λ^{52}, we note that mask μ^3 (which includes the most regular slots) is assigned slightly more often than mask μ^1 (which includes the fewest regular slots), compared to scenario set Λ^{13}. We explain this with the fact that mask μ^1 based on scenario set Λ^{52} includes less regular slots than mask μ^1 based on scenario set Λ^{13}. At the same time, mask μ^3 based on scenario set Λ^{52} also includes less regular slots than mask μ^3 based on scenario set Λ^{13} for patient configurations $1-12$. We conclude this section with an example of a mask, a robust mask, and a robust nested multimask resulted from the tenth run of
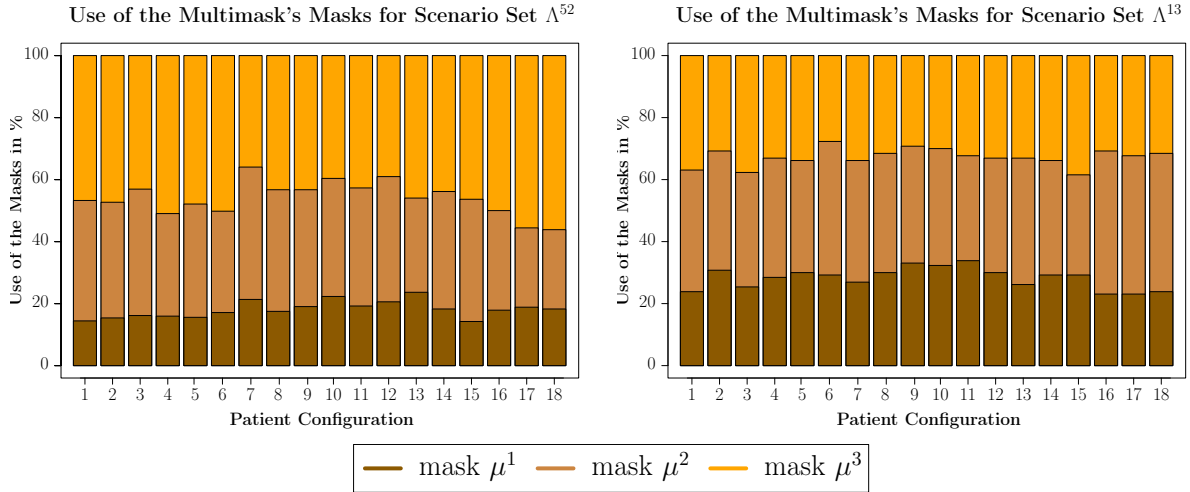
Figure 8: Percentage use of masks μ^1, μ^2, and μ^3

patient configuration 8 as visualized in Figure 9. Considering the results, we note that,
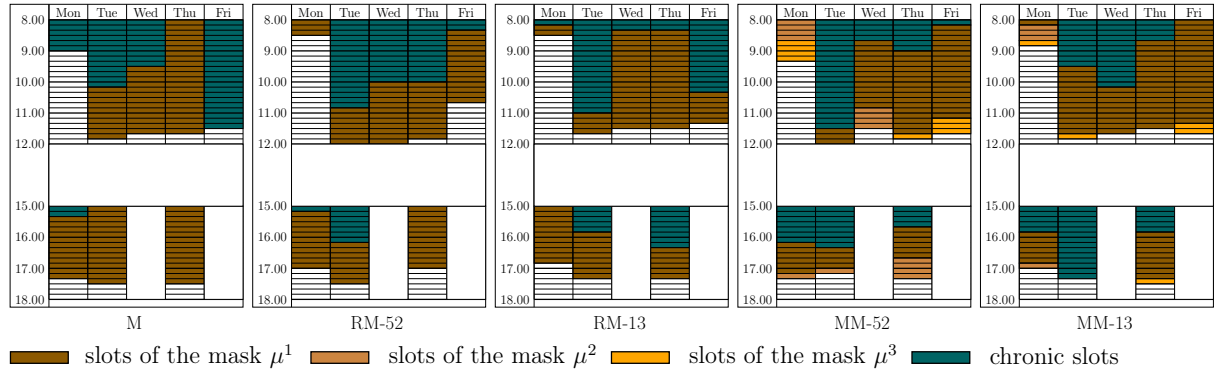
Figure 9: The resulting mask, robust mask, and robust nested mask of the tenth run for patient configuration 8

interestingly, the choice of a robust model corresponding to RM and MM instead of the deterministic model corresponding to M has influenced the positioning of the chronic slots. The robust models account for regular demand before and after the weekend.

6.4 Evaluation by agent-based simulation

In this section, we evaluate the appointment scheduling systems presented in Section 6.1.4. We recall that considering the AM, the HM, and the AA system help as a benchmark. We focus on the comparison of the IBFI and the 2B system with the mask-based systems M, RM, and MM. For the RM and MM appointment scheduling system, we denote whether they are computed on scenario set Λ^{52} or Λ^{13} by RM-52 or RM-13 and MM-52 or MM-13, respectively. In the following, we address RM-52, RM-13, MM-52, and MM-13 as individual appointment scheduling systems. To evaluate the total of ten resulting appointment scheduling systems, we use some of SiM-Care's key performance indicators. For each individual key performance indicator, we summarize the average results of all appointment scheduling systems in Tables 8–17 in Appendix B. In addition, for each individual
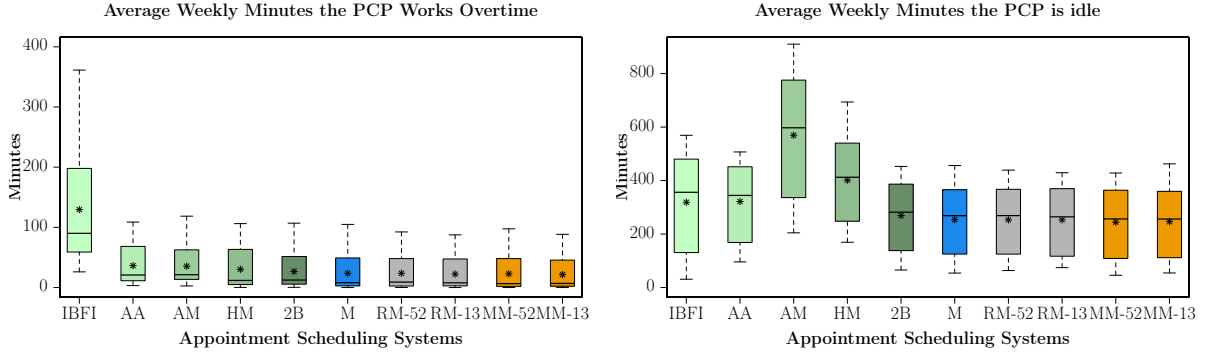
Figure 10: PCP's average weekly overtime and idle time

key performance indicator, we visualize below the results for all appointment scheduling systems of all 180 instances by means of box plots where the average is indicated by a star. We note that the tables and figures are colored by appointment scheduling system. The non-mask-based systems are colored in various shades of green and the mask-based systems in the colors of the underlying optimization problem.

We start with evaluating three key performance indicators for the PCP: the average weekly overtime, the average weekly idle time, and the weekly maximum deviation from the actual to the optimal workload. The results of overtime and idle time are visualized in Figure 10. We confirm that IBFI causes significantly more weekly overtime than all other appointment scheduling systems. The overtime averages 129.48 minutes. These results are consistent with our expectations as IBFI does not reserve time for potential walk-ins. The remaining appointment scheduling systems cause overtime at lower level, which averages between 21.47 and 36.32 minutes. In particular, we note that the mask-based systems perform as well as, and even slightly better than, the non-masked-based systems. We confirm that MM-13 causes the least amount of average overtime at 21.47 minutes. Overall, we note that the average overtime is relatively low which can be explained by the incorporated buffers and the admission of patients up to a certain utilization threshold.

Considering the idle time, we confirm that AM causes the most average weekly idle time. However, if we consider idle time in relation to overtime, we rate IBFI as the worst performing system. Overall, MM-52 achieves the lowest average weekly idle time in the amount of 244 minutes. This is an average of 25 minutes less per week than the idle time caused by 2B, which causes the lowest average weekly idle time among the non-masked-based systems. In fact, all mask-based systems outperform 2B by at least 16 minutes less average weekly idle time.

Finally, across all 52 weeks, we consider the worst-case maximum deviation of the actual from the optimal PCP's workload among all sessions as visualized in Figure 11. This corresponds to the definition of the cost of a (robust) mask for the mask-based systems. IBFI causes the largest average worst-case imbalance between the actual and optimal PCP's workload. This average imbalance is only minimally larger than that caused by AM. Based on the results of overtime and idle time, these results are consistent with our expectations. We further note that AA causes the maximum worst-case deviation of 0.83, i.e., the PCP works 0.83 times the optimal workload more or less in a session. If we consider the non-mask-based systems, we confirm that 2B performs best on average but also in general. In addition, 2B performs better than M but on average worse than
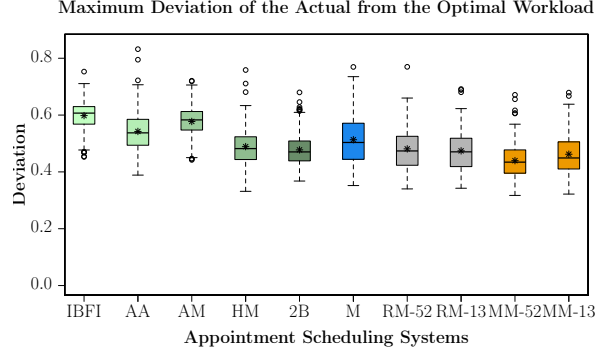
Figure 11: Worst-case deviations of the 52 weeks of all instances, i.e., in each case the worst-case deviation of the actual from the optimal PCP's workload among all sessions
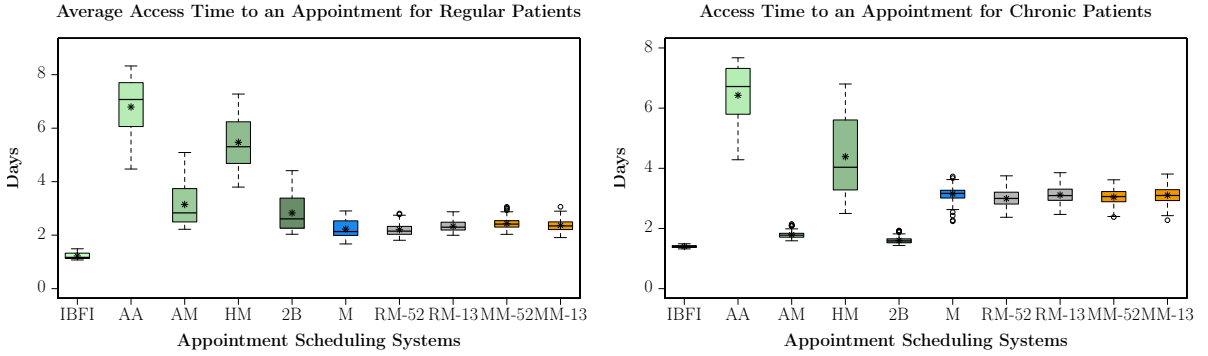
Figure 12: Access time to an appointment for regular and chronic patients

all other mask-based systems. Overall, MM-52 causes the smallest average worst-case deviation of 0.46. Among all appointment scheduling systems, it also causes the smallest maximum worst-case deviation. In conclusion, compared to the appointment scheduling systems from the literature, the mask-based systems achieve to balance the utilization of the PCP 's capacity as targeted in Section 3.3.

In the next step, we consider seven key performance indicators for patients. First, we discuss the access time to an appointment of regular and chronic patients as visualized in Figure 12. As expected, IBFI ensures the shortest access time to an appointment for regular and chronic patients. For instance, for regular patients, the maximum and average access times to an appointment are 1.49 and 1.22 days, respectively. Clearly, the benchmark systems AA, AM, HM perform the worst as the slots that allow to accommodate appointments are limited to specific sessions. We confirm that the mask-based systems ensure a faster average access time to an appointment, ranging from 2.20 to 2.43 days, than the 2B system with 2.83 days. However, the average access time to an appointment increases for chronic patients if a mask-based system is used compared to 2B. We explain this by the fact that the mask-based systems distinguish between slots for regular and chronic patients, so fewer appointments are available for chronic patients. Thus, the mask-based systems use the flexibility that chronic patients have. We point out that the timely access for chronic patients is still ensured. Conversely, if there is no distinction between slots for regular and chronic patients, the access time for appointments of chronic patients decreases, as chronic patients are typically scheduled much further in advance.
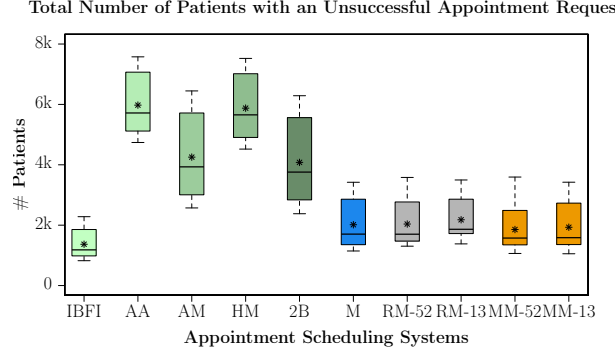
Figure 13: Number of patients with an unsuccessful appointment request

This in turn affects the access time to an appointment for regular patients. We assume that this has occurred for AM and 2B. In conclusion, the mask-based systems ensure for all instances a maximum access time to an appointment for regular and chronic patients of three and four days, respectively. At this point, we emphasize that these access times are guaranteed, although in SiM-Care the patients' willingness to wait is not limited to three days as assumed in the optimization models. Consequently, this meets the objectives formulated in Section 3.1.

Second, we consider the total number of unsuccessful appointment requests within a year as visualized in Figure 13. As IBFI allows all slots to accommodate an appointment, it clearly ensures the smallest number of unsuccessful appointment requests. The results of the benchmark appointment scheduling systems AA, AM, and HM confirm that the number of unsuccessful appointment requests increases if appointment slots are restricted to specific sessions or possibly if too few slots exist that allow to accommodate an appointment. We underline that the mask-based systems perform significantly better than 2B. MM-52 causes a maximum of 3594 unsuccessful appointment requests which is the maximum number among all mask-based systems and still lower than 4080.11 which is the average number of 2B. Furthermore, MM-52 causes with 1855.33 the smallest average number of unsuccessful appointment requests among all mask-based systems and the second smallest average number among all appointment scheduling systems. Overall, we assess that the number of unsuccessful appointment requests is minimized as targeted in the second optimization stage of the optimization models.

Third, we consider the total number of rejected walk-ins within a year, i.e., patients that are not seen by the PCP, and how many of them previously had an unsuccessful appointment request. We note that patients with an appointment are always admitted as long as they arrive before the end of the buffer. Furthermore, we note that the admission strategy in SiM-Care does not favor walk-ins who previously had an unsuccessful appointment request over walk-ins who had not requested an appointment. Accordingly, it is random how many patients are rejected twice, once for an appointment request and once for the treatment itself. Nevertheless, it is interesting to evaluate how many patients are rejected twice by the (appointment scheduling) system. The results are visualized in Figure 14. As IBFI does not reserve slots for potential walk-ins, clearly, it is the system with the highest average total number of rejected walk-ins, namely 213 walk-ins. At the same time, IBFI is the system with the highest average number of rejected walk-ins who previously requested an appointment even though it is the systems with the fewest aver-
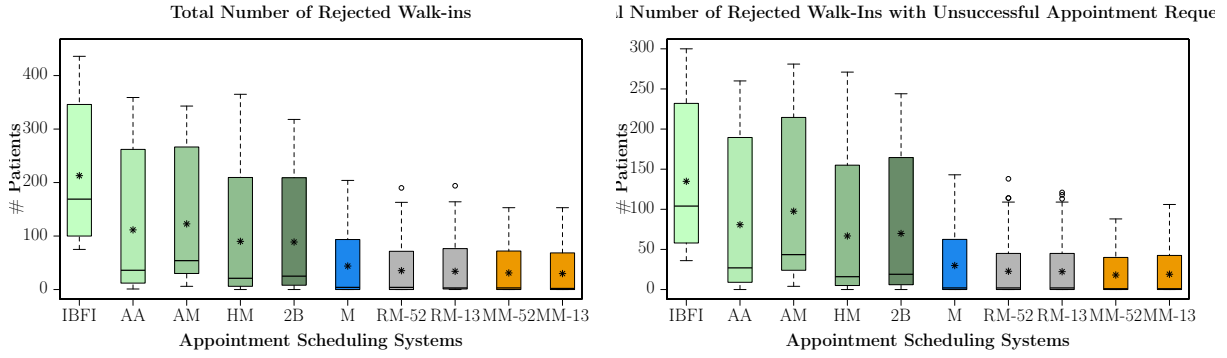
Figure 14: Number of rejected walk-ins and how many of them previously had an unsuccessful appointment request

age unsuccessful appointment requests. It is also noticeable that the benchmark systems AA, AM, HM and even 2B reject more than twice as many patients on average than the mask-based systems. More precisely, 2B rejects 89 walk-ins on average while the mask-based systems M, RM-52, RM-13, MM-52, and MM-13 reject 44, 35, 34, 31, 30 walk-ins on average, respectively. Furthermore, the maximum and average numbers for the rejected walk-ins who previously had an unsuccessful appointment request are on a lower level for the mask-based systems compared to the non-mask-based systems. Overall, the mask-based systems cause fewer unsuccessful appointment requests, fewer rejected walk-ins, and thus fewer walk-ins who have previously requested an appointment, compared to all other appointment scheduling systems.

Finally, we consider the average waiting times for treatments in the practice for patients with appointments and walk-ins. The results are visualized in Figure 15. As the treatment strategy is defined so that patients with appointments are always prioritized over walk-ins in the treatment order, waiting times for walk-ins are significantly higher than those from patients with appointments. Considering the waiting times for patients with appointments first, we see that the benchmark systems AA, AM, HM perform the best with an average waiting time ranging between 3.42 and 3.53 minutes. The average waiting times caused by the mask-based systems are comparable to the average waiting time of 6.32 minutes caused by IBFI, they are only 0.09 minutes longer. Neglecting the
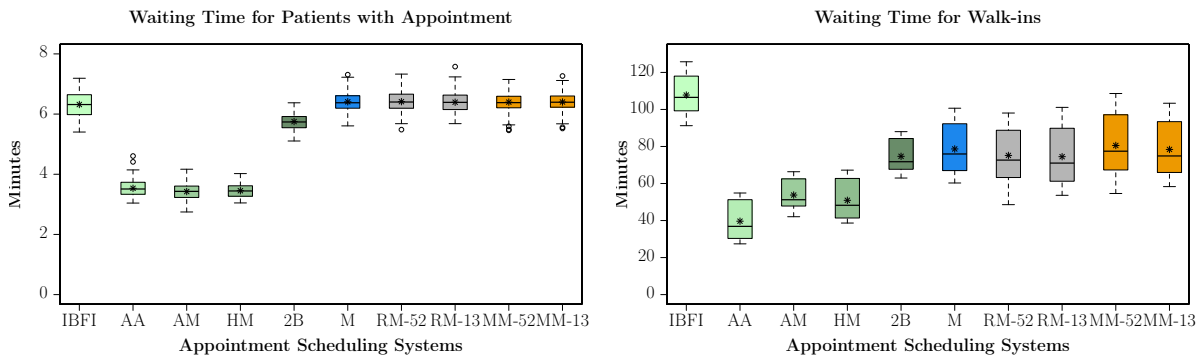
Figure 15: Waiting time for treatment within the practice of patients with appointment and walk-ins

benchmark systems, we confirm that 2B causes with 5.75 minutes the lowest average waiting times for patients with appointments. Considering the waiting times of walk-ins next, we see that the benchmark systems perform again the best with an average waiting time ranging between 39.65 and 53.77 minutes. 2B provides with 74.68 minutes the next lowest average waiting time for walk-ins. The mask-based systems cause worse, but similarly good average waiting times for walk-ins than 2B ranging between 74.49 and 80.54 minutes. We note that MM-52, which causes the maximum waiting time among all mask-based systems, causes only 0.83 minutes more waiting time than the average waiting time caused IBFI. Furthermore, we note that the maximum waiting time which a walk-in has to wait among all appointment scheduling strategies is caused by IBFI with 125.75 minutes. We conclude this section and refer to the next section where we summarize the results of the mask-based systems and assess them among each other.

7   Discussion and conclusion

In this paper, we managed a PCP's demand for treatment considering three different types of patients by interday appointment scheduling on a tactical decision level. We introduced the MDP and provided a combinatorial interpretation by a network flow and design model. Furthermore, we extended the MDP to the rMDP to obtain a robust setting in which we could account for uncertainties in the weekly distributions of demand. To avoid overfitted solutions and to prevent uncertainties not only in the weekly distribution but also in the total demand, we introduced the rMMDP. For all three problems, we developed a solution approach that combined binary search with compact IP formulations of extension of minimum cost flow problems. We analyzed the optimization models and discussed their results. Finally, we conducted an extensive case study by agent-based simulation in which we evaluated the resulting mask-based appointment scheduling systems and compared them with five appointment scheduling systems from the literature.

Compared to the presented appointment scheduling systems from the literature, our study shows the potential of the mask-based appointment scheduling systems. The mask-based appointment scheduling systems improve the balanced utilization of the PCP, identifiable by the minimized overtime, idle time, and worst-case deviation of the actual from the optimal workload. Furthermore, they ensure the (timely) access to medical care which includes the following three aspects. First, more patients may receive an appointment so that there are fewer unsuccessful appointment requests. Second, the timely access to an appointment is ensured for regular patients within three days and for chronic patients within four days. Third, more patients are admitted for treatment and consequently fewer patients are rejected. We point out that the timely access comes at the expenses of waiting times within the practice. To overcome this deficit, future work needs to investigate the order of slots with specific states, especially the positioning of the walk-in slots. Since the walk-in slots are always positioned at the end of a session in the presented appointment scheduling systems, it is not surprising that walk-ins have long waiting times to their treatments. In addition to the positioning of the walk-in slots, walk-ins' waiting times can be beneficially controlled by an adjusted treatment strategy that does not always prioritize patients with appointments over walk-ins.

While this study represents a valuable contribution for interday appointment scheduling in primary care practices, we must not overlook the major limitations of our models and our case study that stem from assumptions and open up directions for further re-

search. Concerning the limitations of our models, we note our assumption that patients always attend their appointments. The exclusion of potential no-shows is quite strict and definitely not true in reality. To overcome this limitation in future work, we might integrate no-shows in our models by additional sink vertices between the appointment and treatment arcs that demand a number of no-shows. Naturally, we would then also integrate no-shows into the simulation model. Concerning the limitations of our case study, we note that the lack of empirical demand data forced us to use a simulation model which can provide rough estimates at best. Furthermore, we could not sufficiently clarify on which scenario set the mask-based appointment scheduling systems work better. The question could be answered depending on available demand data and available time for computation.

Overall, we obtain the following four key findings of this study. First, the distinction in slots reserved for specific patient types is beneficially for the demand management. Second, taking into account information like high walk-in rates in specific sessions has a major impact on the resulting appointment scheduling system and should thus be considered in interday appointment scheduling. Third, a robust nested multimask may be advantageous over a robust mask as observable in key performance indicators such as the number of patients with an unsuccessful appointment request, the number of rejected walk-ins, and the number of rejected patients who previously had an unsuccessful appointment request. We also confirm better results regarding the maximum deviation of the actual from the optimal workload of the PCP. In future research, however, we need to investigate the circumstances under which appointments of the second and third mask of the multimask are offered to the patients to fully realize the potential of a multimask. Fourth, our robust and combinatorial network flow and design models are applicable and effective methods to manage demand in primary care practices. More precisely, they are valid modelings for interday appointment scheduling on a tactical decision level. In addition, they withstand a much more complex simulation model on an operational level. We conclude this paper with the confidence that our mask-based appointment scheduling systems meet the effectiveness described in the introduction at the beginning of the paper: The mask-based appointment scheduling systems maintain patient-physician continuity, enable timely access, reduce waiting times, smooth the PCP workflow, and provide robustness against demand uncertainties.

References

[1] IBM (2018). IBM CPLEX Optimization Studio 22.1.0.

[2] Amir Ahmadi-Javid, Zahra Jalali, and Kenneth J Klassen. Outpatient appointment systems in healthcare: A review of optimization studies. *European Journal of Operational Research*, 258(1):3–34, 2017.

[3] Berhanu Alemayehu and Kenneth E Warner. The lifetime distribution of health care costs. *Health services research*, 39(3):627–642, 2004.

[4] Roger Anderson, Angela Barbara, Steven Feldman, et al. What patients want: a content analysis of key qualities that influence patient satisfaction. *J Med Pract Manage*, 22(5):255–261, 2007.

[5] Statistische Informationen aus dem Bundesarztregister. Kassenärztliche Bundesvereinigung (2017).

[6] H. Balasubramanian, S. Biehl, L. Dai, and A. Muriel. Dynamic allocation of same-day requests in multi-physician primary care practices in the presence of prescheduled appointments. *Health Care Management Science*, 17(1):31–48, 2014.

[7] Hari Balasubramanian, Ana Muriel, and Liang Wang. The impact of provider flexibility and capacity allocation on the performance of primary care practices. *Flexible Services and Manufacturing Journal*, 24(4):422–447, 2012.

[8] Dimitris Bertsimas and Melvyn Sim. The price of robustness. *Operations research*, 52(1):35–53, 2004.

[9] Thomas Bodenheimer. Primary care — will it survive? *New England Journal of Medicine*, 355(9):861–864, 2006. PMID: 16943396.

[10] Kassenärztliche Bundesvereinigung.

[11] Christina Büsing, Arie MCA Koster, and Sabrina Schmitz. Robust minimum cost flow problem under consistent flow constraints. *Annals of Operations Research*, 312(2):691–722, 2022.

[12] T. Cayirli and E. Veral. Outpatient scheduling in health care: A review of literature. *Production and Operations Management*, 12(4):519–549, 2003.

[13] Tugba Cayirli and Evrim Didem Gunes. Outpatient appointment scheduling in presence of seasonal walk-ins. *Journal of the Operational Research Society*, 65(4):512–531, 2014.

[14] Jack M. Colwill, James M. Cultice, and Robin L. Kruse. Will generalist physician supply meet demands of an increasing and aging population? *Health Affairs*, 27(3):w232–w241, 2008. PMID: 18445642.

[15] Martin Comis, Catherine Cleophas, and Christina Büsing. Patients, primary care, and policy: Agent-based simulation modeling for health care decision support. *Health Care Management Science*, pages 1–28, 2021.

[16] Federal Joint Commitee.

[17] Bundesministerium der Justiz und für Verbraucherschutz.

[18] Gregory Dobson, Sameer Hasija, and Edieal J Pinker. Reserving capacity for urgent patients in primary care. *Production and Operations Management*, 20(3):456–473, 2011.

[19] Jacob Feldman, Nan Liu, Huseyin Topaloglu, and Serhan Ziya. Appointment scheduling under patient preference and no-show behavior. *Operations Research*, 62(4):794–811, 2014.

[20] GKV-Spitzenverband.

[21] Anders N Gullhav, Marielle Christiansen, Bjørn Nygreen, Mats M Aarlott, Jon Erik Medhus, Johan Fredrik Skomsvoll, and Per Olav Østbyhaug. Block scheduling at magnetic resonance imaging labs. *Operations Research for Health Care*, 18:52–64, 2018.

[22] D. Gupta and B. Denton. Appointment scheduling in health care: Challenges and opportunities. *IIE transactions*, 40(9):800–819, 2008.

[23] Paul Robert Harper and HM Gamlin. Reduced outpatient waiting times with improved appointment scheduling: a simulation modelling approach. *Or Spectrum*, 25(2):207–222, 2003.

[24] Babak Hoseini, Wenbo Cai, and Layek Abdel-Malek. A carve-out model for primary care appointment scheduling with same-day requests and no-shows. *Operations research for health care*, 16:41–58, 2018.

[25] Xiao-Ming Huang. Patient attitude towards waiting in an outpatient clinic and its applications. *Health Services Management Research*, 7(1):2–8, 1994.

[26] Y Huang and P Zuniga. Dynamic overbooking scheduling system to improve patient access. *Journal of the Operational Research Society*, 63(6):810–820, 2012.

[27] P. J. H. Hulshof, N. Kortbeek, R. J. Boucherie, E. W. Hans, and P. J. M. Bakker. Taxonomic classification of planning decisions in health care: a structured review of the state of the art in or/ms. *Health Systems*, 1(2):129–175, 2012.

[28] Gesundheit in Deutschland aktuell 2010.

[29] Rüdiger Jacob, J Kopp, and S Schultz. Berufsmonitoring medizinstudenten 2014. *Ergebnisse einer bundesweiten Befragung. Berlin: KBV, Kassenärztliche Bundesvereinigung*, 2015.

[30] Kassenärtzliche Vereinigung Nordrhein. Die 100 häufigsten ICD-10-Schlüssel und Kurztexte (nach Fachgruppen) - 4. Quartal 2018. pages 1–125, 2018.

[31] Seongmoon Kim and Ronald E Giachetti. A stochastic mathematical appointment overbooking model for healthcare providers to improve profits. *IEEE Transactions on systems, man, and cybernetics-Part A: Systems and humans*, 36(6):1211–1219, 2006.

[32] Song-Hee Kim, Carri W Chan, Marcelo Olivares, and Gabriel Escobar. Icu admission control: An empirical study of capacity allocation and its implication for patient outcomes. *Management Science*, 61(1):19–38, 2015.

[33] Oracle (2018). Open Java Development Kit.

[34] K. J. Klassen and T. R. Rohleder. Scheduling outpatient appointments in a dynamic environment. *Journal of Operations Management*, 14(2):83 – 101, 1996.

[35] Bernhard Korte, Jens Vygen, B Korte, and J Vygen. *Combinatorial optimization*, volume 2. Springer, 2012.

[36] Linda R LaGanga and Stephen R Lawrence. Clinic overbooking to improve patient access and increase provider productivity. *Decision Sciences*, 38(2):251–276, 2007.

[37] Linda R LaGanga and Stephen R Lawrence. Appointment overbooking in health care clinics to improve patient service and clinic performance. *Production and Operations Management*, 21(5):874–888, 2012.

[38] E Mann, B Schuetz, and E Rubin-Johnston. Remaking primary care: A framework for the future (new england healthcare institute report), 2010.

[39] David Mechanic, Donna D McAlpine, and Marsha Rosenthal. Are patients' office visits with physicians getting shorter? *New England Journal of Medicine*, 344(3):198–204, 2001.

[40] Mark Murray and Donald M Berwick. Advanced access: reducing waiting and delays in primary care. *Jama*, 289(8):1035–1040, 2003.

[41] American Academy of Family Physicians (2019) Primary care.

[42] The Associations of Statutory Health Insurance Physicians.

[43] Ann S O'Malley and Peter J Cunningham. Patient experiences with coordination of care: the benefit of continuity and primary care physician as referral source. *Journal of general internal medicine*, 24:170–177, 2009.

[44] Yidong Peng, Xiuli Qu, and Jing Shi. A hybrid simulation and genetic algorithm approach to determine the optimal scheduling templates for open access clinics admitting walk-in patients. *Computers & Industrial Engineering*, 72:282–296, 2014.

[45] X. Qu, Y. Peng, J. Shi, and L. LaGanga. An mdp model for walk-in patient admission management in primary care clinics. *International Journal of Production Economics*, 168:303–320, 2015.

[46] Xiuli Qu, Ronald L Rardin, and Julie Ann S Williams. Single versus hybrid time horizons for open access scheduling. *Computers & Industrial Engineering*, 60(1):56–65, 2011.

[47] Xiuli Qu, Ronald L Rardin, and Julie Ann S Williams. A mean–variance model to optimize the fixed versus open appointment percentages in open access scheduling systems. *Decision Support Systems*, 53(3):554–564, 2012.

[48] Xiuli Qu, Ronald L Rardin, Julie Ann S Williams, and Deanna R Willis. Matching daily healthcare provider capacity to demand in advanced access scheduling systems. *European Journal of Operational Research*, 183(2):812–826, 2007.

[49] Lawrence W Robinson and Rachel R Chen. A comparison of traditional and open-access policies for appointment scheduling. *Manufacturing & Service Operations Management*, 12(2):330–346, 2010.

[50] George Staben Rust, Jiali Ye, Peter A. Baltrus, Elvan Daniels, Bamidele A. Adesunloye, and George Edward Fryer. Practical barriers to timely primary care access: impact on adult use of emergency department services. *Archives of internal medicine*, 168 15:1705–10, 2008.

[51] Matthias Schacht. Improving same-day access in primary care: Optimal reconfiguration of appointment system setups. *Operations Research for Health Care*, 18:119–134, 2018.

[52] Ming Tai-Seale, Thomas G McGuire, and Weimin Zhang. Time allocation in primary care office visits. *Health services research*, 42(5):1871–1894, 2007.

[53] Wen-Ya Wang and Diwakar Gupta. Adaptive appointment systems with patient preferences. *Manufacturing & Service Operations Management*, 13(3):373–389, 2011.

[54] L. Wiesche, M. Schacht, and B. Werners. Strategies for interday appointment scheduling in primary care. *Health care management science*, pages 1–16, 2016.

[55] A. Wolfe. Institute of medicine report: Crossing the quality chasm: A new health care system for the 21st century. *Policy, Politics, & Nursing Practice*, 2(3):233–235, 2001.

[56] Bichen Zheng, Sang Won Yoon, Mohammad T Khasawneh, et al. An overbooking scheduling model for outpatient appointments in a multi-provider clinic. *Operations Research for Health Care*, 6:1–10, 2015.

A Algorithm 1

In this section, we present the omitted Algorithm 1.

Algorithm 1

Input: Network $N = (G, \overline{\psi}, \beta)$

Output: Feasible β-flow in network N_ω with minimum $\omega \in \Omega$

Method:

> Set $\omega_{\text{LB}} = 0$ and $\omega_{\text{UB}} = \max\limits_{k \in \mathcal{K}} D_k$
> **while** $\omega_{\text{LB}} \neq \omega_{\text{UB}}$ **do**
>> Compute $\widetilde{\omega} = \lfloor \frac{\omega_{\text{LB}} + \omega_{\text{UB}}}{2} \rfloor$
>> Set $\overline{\omega} = \widetilde{\omega} \cdot t$
>> **if** there exists a feasible β-flow $f_{\overline{\omega}}$ in network $N_{\overline{\omega}}$ **then**
>>> Update $\omega_{\text{UB}} = \widetilde{\omega}$ and set $f = f_{\overline{\omega}}$
>>
>> **else**
>>> Update $\omega_{\text{UB}} = \widetilde{\omega} + 1$
>>
>> **end if**
>
> **end while**
> Set $\overline{\omega} = \omega_{\text{UB}} \cdot t$
> **for** $k \in \mathcal{K}$ **do**
>> Compute $i_1 = \left\lfloor \frac{\overline{\omega} + u \cdot c_k}{t} \right\rfloor$ and $\omega_{i_1} = |t \cdot i_1 - u \cdot c_k|$
>> Compute $i_2 = \left\lceil \frac{u \cdot c_k - \overline{\omega}}{t} \right\rceil$ and $\omega_{i_2} = |t \cdot i_2 - u \cdot c_k|$
>> **for** $\omega \in \{\omega_{i_1}, \omega_{i_2}\}$ **do**
>>> **if** $\omega < \overline{\omega}$ **then**
>>>> **if** there exists a feasible β-flow f_ω in network N_ω **then**
>>>>> Update $\overline{\omega} = \omega$ and set $f = f_\omega$
>>>>
>>>> **end if**
>>>
>>> **end if**
>>
>> **end for**
>
> **end for**
> **return** $\overline{\omega}$ and β-flow f

B Computational results

In this section, we present the computational results of the optimization problems as well as the average results of the evaluation by simulation.

C-ID	Patient Config.	Run	objective value/ deviation ω			# unsuc. appointment requests $d_w^r(\cdot)$			# regular slots $\sum\limits_{k\in\mathcal{K}} n_\mu(r,k)$			# chronic slots $\sum\limits_{k\in\mathcal{K}} n_\mu(c,k)$	
			Det-F	Rob-F	RobM-F	Det-F	Rob-F	RobM-F	Det-F	Rob-F	RobM-F	Det-F	Rob(M)-F
1	1400/15/40	1	7.8	46.8	23.68	0	208	609	83	78	84	43	44
1	1400/15/40	2	4.25	46.8	20.42	0	260	760	78	73	67	46	44
1	1400/15/40	3	4.25	35.45	19	0	156	684	80	77	75	43	44
1	1400/15/40	4	4.25	57.44	25.81	0	156	776	80	76	73	44	44
1	1400/15/40	5	4.96	27.65	20.99	0	156	473	80	77	76	42	44
1	1400/15/40	6	4.25	43.25	33.19	0	104	374	80	78	76	44	44
1	1400/15/40	7	1.42	39	26.24	0	312	385	82	76	83	44	44
1	1400/15/40	8	4.25	41.84	17.44	0	104	693	81	79	78	43	44
1	1400/15/40	9	4.25	41.84	30.35	0	156	425	80	78	76	44	44
1	1400/15/40	10	6.81	54.46	37.58	0	156	271	79	76	81	45	44
2	1400/18/40	1	6.81	43.25	21.41	0	260	718	79	74	76	43	44
2	1400/18/40	2	5.67	46.66	21.7	0	312	593	74	70	70	46	44
2	1400/18/40	3	4.25	43.25	23.97	0	104	671	76	74	76	43	44
2	1400/18/40	4	5.39	54.46	16.31	0	104	872	76	75	68	43	44
2	1400/18/40	5	4.25	38.01	20.99	0	208	521	77	73	74	43	44
2	1400/18/40	6	6.81	42.55	26.95	0	104	304	77	75	81	44	44
2	1400/18/40	7	7.8	49.64	26.24	0	364	412	81	72	78	43	44
2	1400/18/40	8	7.8	41.84	18.15	0	156	617	79	76	75	45	44
2	1400/18/40	9	7.8	54.6	31.34	0	52	404	79	77	74	44	44
2	1400/18/40	10	6.81	62.26	36.16	0	104	343	75	74	73	46	44
3	1400/20/40	1	4.25	51.05	20.28	0	208	829	78	73	73	43	44
3	1400/20/40	2	6.81	46.8	21.7	0	208	549	74	70	71	46	44
3	1400/20/40	3	4.25	46.8	31.77	0	104	361	75	73	78	43	44
3	1400/20/40	4	6.81	57.44	18.58	0	104	923	75	73	63	44	44
3	1400/20/40	5	4.96	34.75	28.79	0	312	392	76	69	71	42	44
3	1400/20/40	6	7.8	34.75	34.75	0	260	276	76	70	78	44	44
3	1400/20/40	7	4.25	48.93	26.24	0	312	406	78	72	79	43	44
3	1400/20/40	8	4.96	49.64	25.24	0	104	415	75	75	82	44	44
3	1400/20/40	9	4.25	57.44	39.14	0	104	361	76	74	76	44	44
3	1400/20/40	10	4.25	54.46	28.36	0	156	367	74	71	75	46	44
4	1400/15/45	1	7.8	46.8	22.97	0	52	499	79	79	82	49	49
4	1400/15/45	2	7.8	47.93	69.92	0	156	202	77	74	78	50	50
4	1400/15/45	3	6.67	28.93	16.59	0	468	891	78	70	66	50	50
4	1400/15/45	4	1.42	46.8	26.52	0	156	520	77	74	70	48	49
4	1400/15/45	5	7.8	39	45.38	0	156	405	79	77	74	50	49
4	1400/15/45	6	7.8	50.2	58.85	0	208	278	80	77	79	49	49
4	1400/15/45	7	6.67	37.87	20.56	0	312	579	80	74	75	51	50
4	1400/15/45	8	5.53	45.67	17.73	0	260	916	80	75	74	51	49
4	1400/15/45	9	6.67	46.8	18.44	0	52	743	79	78	77	52	50
4	1400/15/45	10	1.42	63.53	31.91	0	0	585	78	78	76	50	50
5	1400/18/45	1	5.53	39	18.44	0	104	760	78	76	77	50	49
5	1400/18/45	2	6.67	48.22	62.12	0	156	180	74	71	75	50	50
5	1400/18/45	3	6.67	28.93	18.44	0	364	760	75	69	68	50	50
5	1400/18/45	4	6.67	40.42	23.54	0	156	652	75	71	66	49	49
5	1400/18/45	5	6.67	46.8	41.98	0	104	383	77	75	73	50	50
5	1400/18/45	6	5.53	52.47	57.72	0	260	250	78	74	80	49	49
5	1400/18/45	7	5.53	45.67	20.71	0	260	603	78	73	74	50	50
5	1400/18/45	8	5.53	39	22.41	0	312	558	77	71	73	51	49
5	1400/18/45	9	6.67	54.6	26.24	0	104	481	76	74	78	51	50
5	1400/18/45	10	7.8	56.02	30.77	0	104	567	76	73	74	50	50
6	1400/20/45	1	6.67	46.8	18.86	0	52	701	75	75	75	50	49
6	1400/20/45	2	6.67	46.09	62.12	0	156	220	74	70	72	50	50
6	1400/20/45	3	6.67	36.73	22.41	0	208	729	74	70	68	50	50
6	1400/20/45	4	1.42	38.29	23.97	0	156	560	75	70	65	48	50
6	1400/20/45	5	6.67	45.67	43.11	0	156	431	77	73	70	50	50
6	1400/20/45	6	4.4	50.2	64.39	0	260	203	78	72	81	49	49
6	1400/20/45	7	4.4	45.67	23.54	0	104	539	76	74	68	51	50
6	1400/20/45	8	5.53	45.67	22.41	0	208	670	75	72	73	51	49
6	1400/20/45	9	7.8	54.6	26.24	0	52	613	74	74	73	51	50
6	1400/20/45	10	1.42	54.6	22.97	0	156	769	74	70	70	49	50

Table 2: Computational results of the mask models for patient configurations $1-6$

C-ID	Patient Config.	Run	objective value/ deviation ω			# unsuc. appointment requests $d_w^r(\cdot)$			# regular slots $\sum\limits_{k\in\mathcal{K}} n_\mu(r,k)$			# chronic slots $\sum\limits_{k\in\mathcal{K}} n_\mu(c,k)$	
			Det-F	Rob-F	RobM-F	Det-F	Rob-F	RobM-F	Det-F	Rob-F	RobM-F	Det-F	Rob(M)-F
7	1600/15/40	1	7.09	55.31	56.59	2	0	481	89	90	96	51	50
7	1600/15/40	2	7.8	48.64	46.37	0	312	286	89	83	88	49	51
7	1600/15/40	3	6.38	41.84	24.68	1	208	745	90	86	84	51	50
7	1600/15/40	4	4.25	51.05	66.65	2	52	348	85	87	98	52	50
7	1600/15/40	5	1.84	47.51	38.86	2	104	321	86	88	90	52	51
7	1600/15/40	6	1.84	41.84	29.5	0	208	384	90	86	90	50	50
7	1600/15/40	7	6.38	34.04	16.59	0	312	772	88	83	88	51	50
7	1600/15/40	8	7.8	78	19.71	2	0	998	89	91	81	50	50
7	1600/15/40	9	1.84	39	27.09	2	676	489	88	75	86	51	51
7	1600/15/40	10	6.38	46.8	39.57	0	520	368	87	79	92	51	51
8	1600/18/40	1	6.24	55.31	48.64	0	0	468	88	87	88	51	50
8	1600/18/40	2	7.8	46.8	46.37	1	312	228	86	81	88	49	51
8	1600/18/40	3	6.38	46.8	29.92	0	156	503	87	84	81	52	50
8	1600/18/40	4	1.84	43.25	67.79	1	208	302	85	82	87	52	50
8	1600/18/40	5	7.09	48.64	47.79	0	104	296	87	85	88	52	51
8	1600/18/40	6	7.8	34.04	37.3	0	312	323	87	81	86	50	50
8	1600/18/40	7	7.8	35.45	13.76	1	208	1066	86	83	73	51	50
8	1600/18/40	8	1.84	62.4	20.71	1	52	1091	87	87	77	49	50
8	1600/18/40	9	6.38	42.55	28.51	0	520	492	85	76	89	51	51
8	1600/18/40	10	7.8	57.44	47.37	0	468	265	87	78	88	51	51
9	1600/20/40	1	1.84	63.11	56.44	0	0	455	84	86	82	51	50
9	1600/20/40	2	4.25	54.6	47.51	0	260	230	84	80	87	49	51
9	1600/20/40	3	6.38	54.6	25.53	0	156	600	86	83	79	50	50
9	1600/20/40	4	7.8	51.05	67.79	0	156	281	84	81	85	51	50
9	1600/20/40	5	6.38	56.44	55.59	0	52	283	85	84	85	52	51
9	1600/20/40	6	7.8	46.8	34.04	0	260	404	84	80	85	50	50
9	1600/20/40	7	6.38	35.45	12.91	0	208	1065	85	81	79	50	50
9	1600/20/40	8	1.84	72.04	18.15	0	0	1175	86	86	76	49	50
9	1600/20/40	9	1.84	39	31.06	0	624	400	84	72	85	51	51
9	1600/20/40	10	6.38	54.6	39.57	0	520	348	85	74	82	52	51
10	1600/15/45	1	7.8	76.44	33.33	2	0	546	87	88	82	57	56
10	1600/15/45	2	6.24	53.18	24.82	2	104	791	85	85	89	55	57
10	1600/15/45	3	5.11	53.04	36.87	1	104	384	86	84	87	55	56
10	1600/15/45	4	6.38	60.98	24.53	1	0	809	88	90	82	57	56
10	1600/15/45	5	6.38	70.2	31.06	2	0	997	84	85	79	57	57
10	1600/15/45	6	7.8	56.73	21.84	2	52	830	87	88	84	57	57
10	1600/15/45	7	6.38	76.58	34.6	1	0	645	88	88	85	56	57
10	1600/15/45	8	7.8	53.18	29.78	3	208	851	87	84	75	57	57
10	1600/15/45	9	6.38	58.43	33.04	1	104	644	88	87	83	56	57
10	1600/15/45	10	6.24	59.71	26.52	1	0	990	87	87	71	55	56
11	1600/18/45	1	6.24	76.44	33.33	1	0	532	84	85	80	56	56
11	1600/18/45	2	6.38	53.18	31.77	1	0	461	84	84	87	55	57
11	1600/18/45	3	6.38	45.24	44.67	0	104	329	84	81	85	55	56
11	1600/18/45	4	6.38	58.43	28.08	1	52	567	86	86	86	57	56
11	1600/18/45	5	6.38	78	31.63	2	0	920	81	83	78	57	57
11	1600/18/45	6	0.57	54.6	38.15	2	208	461	84	82	84	58	57
11	1600/18/45	7	6.38	81.83	36.16	1	0	760	85	85	85	56	57
11	1600/18/45	8	6.38	48.93	36.59	2	312	736	83	80	73	57	57
11	1600/18/45	9	7.09	58.43	33.89	1	156	580	83	83	80	57	57
11	1600/18/45	10	5.11	60.84	26.95	1	0	1047	85	84	69	55	56
12	1600/20/45	1	7.09	76.44	33.33	1	0	557	81	83	77	57	56
12	1600/20/45	2	5.11	50.63	30.77	0	52	494	82	82	85	55	57
12	1600/20/45	3	5.11	53.04	44.67	0	156	314	82	78	83	55	56
12	1600/20/45	4	6.38	62.4	28.51	0	52	597	85	85	81	56	56
12	1600/20/45	5	1.84	70.91	31.77	2	0	929	80	82	74	57	57
12	1600/20/45	6	7.8	54.6	28.36	0	104	812	83	82	81	58	57
12	1600/20/45	7	7.8	84.38	35.45	1	0	727	84	83	82	56	57
12	1600/20/45	8	6.38	48.93	40.42	1	208	727	82	80	71	57	57
12	1600/20/45	9	5.11	60.98	39	1	104	508	84	83	91	56	57
12	1600/20/45	10	5.11	59.71	34.18	0	52	619	82	81	79	55	56

Table 3: Computational results of the mask models for patient configurations $7-12$

C-ID	Patient Config.	Run	objective value/ deviation ω			# unsuc. appointment requests $d_w^r(\cdot)$			# regular slots $\sum_{k\in\mathcal{K}} n_\mu(r,k)$			# chronic slots $\sum_{k\in\mathcal{K}} n_\mu(c,k)$	
			Det-F	Rob-F	RobM-F	Det-F	Rob-F	RobM-F	Det-F	Rob-F	RobM-F	Det-F	Rob(M)-F
13	2000/15/40	1	5.39	81.55	89.49	20	1196	597	83	80	95	63	63
13	2000/15/40	2	5.67	92.61	41.41	19	780	1091	82	86	88	65	63
13	2000/15/40	3	5.67	73.75	34.89	17	936	1217	87	85	91	60	63
13	2000/15/40	4	4.68	60.98	37.16	21	1092	1005	84	84	90	64	62
13	2000/15/40	5	4.96	80.84	57.44	19	1092	853	85	82	90	62	63
13	2000/15/40	6	7.09	69.49	58.71	19	988	777	83	83	90	63	63
13	2000/15/40	7	7.09	77.29	47.08	19	1092	1007	83	81	86	63	63
13	2000/15/40	8	7.09	76.58	46.37	19	884	1053	84	86	87	63	63
13	2000/15/40	9	5.39	81.55	23.12	20	936	1301	83	86	89	64	63
13	2000/15/40	10	4.96	62.4	34.04	17	1040	1004	84	82	89	63	63
14	2000/18/40	1	5.81	72.61	81.69	20	988	529	82	81	94	65	63
14	2000/18/40	2	5.67	84.81	37.3	17	624	1094	82	86	88	64	63
14	2000/18/40	3	4.68	77.29	28.65	16	780	1198	86	86	87	62	63
14	2000/18/40	4	7.09	60.98	44.96	17	936	810	85	84	90	63	62
14	2000/18/40	5	3.55	70.06	40.7	17	1040	915	83	80	87	62	63
14	2000/18/40	6	7.09	77.29	66.37	16	884	595	83	83	92	63	63
14	2000/18/40	7	4.68	73.75	55.03	19	1040	765	81	80	90	64	63
14	2000/18/40	8	5.39	69.49	36.45	18	780	1025	84	86	86	62	63
14	2000/18/40	9	4.68	65.95	32.76	18	832	1045	84	86	88	64	63
14	2000/18/40	10	4.96	57.01	23.97	17	1092	1272	84	80	81	63	63
15	2000/20/40	1	4.68	80.41	82.82	16	884	459	81	81	94	65	63
15	2000/20/40	2	7.09	81.55	43.96	15	572	851	83	86	88	64	63
15	2000/20/40	3	7.09	73.75	52.05	15	728	701	86	85	89	61	63
15	2000/20/40	4	5.81	64.81	48.36	18	1040	739	83	81	91	64	62
15	2000/20/40	5	5.67	73.04	62.97	17	884	631	82	82	92	64	63
15	2000/20/40	6	7.09	77.29	57.44	15	780	595	83	83	91	63	63
15	2000/20/40	7	5.81	89.35	37.58	16	936	1110	82	80	82	63	63
15	2000/20/40	8	5.39	77.29	38.57	16	728	1004	84	85	84	62	63
15	2000/20/40	9	5.39	65.95	36.45	17	832	938	83	84	87	64	63
15	2000/20/40	10	4.68	55.88	31.77	16	1092	1034	84	78	86	63	63
16	2000/15/45	1	7.8	96.15	41.98	19	1196	1280	78	74	78	72	71
16	2000/15/45	2	5.81	92.18	50.77	21	988	966	76	78	86	71	71
16	2000/15/45	3	7.8	85.8	49.64	21	1144	1048	78	76	83	71	71
16	2000/15/45	4	7.8	95.02	47.37	20	1144	1201	77	75	79	72	71
16	2000/15/45	5	2.13	78	36.02	21	1144	1268	76	75	82	72	71
16	2000/15/45	6	7.8	82.82	39.57	19	1196	1130	78	76	80	71	71
16	2000/15/45	7	7.8	95.73	39.85	20	1144	1361	78	75	79	69	71
16	2000/15/45	8	7.8	67.22	41.84	19	1352	1146	78	72	81	71	71
16	2000/15/45	9	4.82	98.42	60.13	21	1144	1426	77	76	72	71	71
16	2000/15/45	10	6.38	84.38	30.77	21	1092	1204	76	76	84	71	71
17	2000/18/45	1	7.8	93.6	45.38	17	1144	1084	78	74	82	72	71
17	2000/18/45	2	6.38	92.18	51.76	19	936	936	77	77	85	70	71
17	2000/18/45	3	4.82	95.02	46.37	21	1092	1034	77	75	82	71	71
17	2000/18/45	4	2.13	101.4	48.5	20	1040	1259	75	75	74	72	71
17	2000/18/45	5	7.8	87.22	42.55	18	1040	1113	76	75	81	72	71
17	2000/18/45	6	4.82	73.75	56.59	21	1040	909	76	77	82	72	71
17	2000/18/45	7	6.38	85.8	35.88	19	1040	1216	77	76	80	69	71
17	2000/18/45	8	7.8	62.4	50.49	18	1248	958	79	72	81	70	71
17	2000/18/45	9	7.8	91.47	52.76	19	1092	1141	77	76	77	70	71
17	2000/18/45	10	2.13	83.81	31.06	21	884	1136	75	77	83	72	71
18	2000/20/45	1	4.82	81.55	43.96	17	1144	1143	78	73	77	72	71
18	2000/20/45	2	5.81	84.38	47.37	17	988	961	78	75	79	69	71
18	2000/20/45	3	7.8	87.22	53.04	18	988	893	76	75	82	71	71
18	2000/20/45	4	7.8	109.2	58.85	18	988	869	76	75	81	71	71
18	2000/20/45	5	7.8	78	41.69	18	936	1075	76	76	79	72	71
18	2000/20/45	6	5.67	70.2	49.64	19	936	912	76	78	84	72	71
18	2000/20/45	7	7.8	78	36.16	20	936	1358	76	77	81	71	71
18	2000/20/45	8	2.13	75.02	40.99	17	1092	1082	78	75	81	69	71
18	2000/20/45	9	4.82	90.62	53.04	19	1040	1196	76	75	74	70	71
18	2000/20/45	10	5.81	83.81	34.75	18	832	921	74	77	82	72	71

Table 4: Computational results of the mask models for patient configurations $13 - 18$

C-ID	Patient Config.	Run	objective value/ deviation ω			# unsuc. appointment requests $d^r_w(\cdot)$			# regular slots $\sum_{k\in\mathcal{K}} n_\mu(r,k)$			# chronic slots $\sum_{k\in\mathcal{K}} n_\mu(c,k)$	
			Det-F	Rob-F	RobM-F	Det-F	Rob-F	RobM-F	Det-F	Rob-F	RobM-F	Det-F	Rob(M)-F
1	1400/15/40	1	7.8	7.8	6.38	0	156	81	83	70	84	43	44
1	1400/15/40	2	4.25	4.96	6.38	0	221	86	78	61	77	46	44
1	1400/15/40	3	4.25	7.8	6.38	0	169	86	80	67	78	43	44
1	1400/15/40	4	4.25	6.81	7.09	0	156	80	80	68	80	44	44
1	1400/15/40	5	4.96	4.25	6.52	0	91	73	80	73	79	42	44
1	1400/15/40	6	4.25	4.25	6.38	0	117	67	80	71	80	44	44
1	1400/15/40	7	1.42	7.8	6.38	0	156	74	82	71	82	44	44
1	1400/15/40	8	4.25	4.25	6.38	0	104	70	81	74	80	43	43
1	1400/15/40	9	4.25	7.8	6.52	0	143	77	80	70	80	44	44
1	1400/15/40	10	6.81	4.96	6.52	0	156	87	79	67	80	45	44
2	1400/18/40	1	6.81	7.8	6.38	0	117	76	79	70	83	43	44
2	1400/18/40	2	5.67	7.66	6.38	0	143	104	74	65	73	46	44
2	1400/18/40	3	4.25	4.25	6.67	0	169	85	76	63	77	43	44
2	1400/18/40	4	5.39	4.96	6.52	0	195	95	76	62	73	43	44
2	1400/18/40	5	4.25	6.81	5.39	0	104	100	77	69	76	43	44
2	1400/18/40	6	6.81	7.8	6.52	0	156	89	77	65	81	44	45
2	1400/18/40	7	7.8	7.8	6.52	0	143	90	81	68	83	43	44
2	1400/18/40	8	7.8	4.25	6.52	0	130	86	79	68	77	45	44
2	1400/18/40	9	7.8	7.8	6.67	0	182	78	79	64	79	44	44
2	1400/18/40	10	6.81	6.81	6.67	0	104	82	75	69	78	46	44
3	1400/20/40	1	4.25	4.25	6.38	0	117	92	78	68	78	43	44
3	1400/20/40	2	6.81	6.81	6.52	0	169	92	74	61	73	46	45
3	1400/20/40	3	4.25	7.8	6.52	0	169	102	75	62	75	43	44
3	1400/20/40	4	6.81	4.96	6.52	0	221	110	75	58	73	44	44
3	1400/20/40	5	4.96	6.81	6.38	0	117	89	76	66	72	42	44
3	1400/20/40	6	7.8	6.81	5.39	0	104	75	76	67	74	44	44
3	1400/20/40	7	4.25	7.8	6.52	0	156	72	78	66	77	43	44
3	1400/20/40	8	4.96	7.8	6.67	0	117	65	75	68	76	44	44
3	1400/20/40	9	4.25	7.8	6.38	0	156	78	76	65	78	44	44
3	1400/20/40	10	4.25	4.25	6.38	0	143	84	74	64	72	46	45
4	1400/15/45	1	7.8	14.47	6.67	0	65	85	79	75	79	49	50
4	1400/15/45	2	7.8	1.42	6.67	0	169	78	77	63	76	50	50
4	1400/15/45	3	6.67	5.53	6.38	0	156	73	78	67	80	50	50
4	1400/15/45	4	1.42	9.22	6.38	0	52	63	77	73	77	48	49
4	1400/15/45	5	7.8	6.67	6.52	0	130	67	79	69	81	50	49
4	1400/15/45	6	7.8	7.8	6.38	0	143	67	80	71	81	49	49
4	1400/15/45	7	6.67	5.53	6.38	0	91	57	80	74	82	51	50
4	1400/15/45	8	5.53	6.67	6.67	0	117	101	80	71	77	51	49
4	1400/15/45	9	6.67	7.8	6.38	0	91	68	79	72	78	52	50
4	1400/15/45	10	1.42	1.42	6.67	0	169	74	78	64	79	50	50
5	1400/18/45	1	5.53	7.8	6.67	0	117	96	78	69	78	50	49
5	1400/18/45	2	6.67	7.8	6.67	0	117	63	74	65	74	50	50
5	1400/18/45	3	6.67	5.53	6.67	0	143	89	75	65	80	50	50
5	1400/18/45	4	6.67	1.42	6.38	0	169	83	75	61	73	49	50
5	1400/18/45	5	6.67	6.67	6.38	0	156	97	77	65	74	50	49
5	1400/18/45	6	5.53	11.2	6.38	0	104	99	78	71	76	49	49
5	1400/18/45	7	5.53	6.67	6.38	0	65	79	78	73	77	50	50
5	1400/18/45	8	5.53	7.8	6.52	0	117	102	77	68	77	51	49
5	1400/18/45	9	6.67	7.8	6.38	0	78	67	76	70	77	51	50
5	1400/18/45	10	7.8	7.8	6.67	0	117	71	76	66	76	50	50
6	1400/20/45	1	6.67	7.8	6.67	0	130	96	75	66	77	50	49
6	1400/20/45	2	6.67	1.42	6.67	0	130	65	74	62	72	50	50
6	1400/20/45	3	6.67	5.53	6.52	0	169	112	74	61	72	50	50
6	1400/20/45	4	1.42	1.42	6.52	0	156	77	75	61	73	48	49
6	1400/20/45	5	6.67	7.8	6.38	0	91	108	77	69	81	50	49
6	1400/20/45	6	4.4	13.47	6.38	0	65	96	78	72	77	49	49
6	1400/20/45	7	4.4	6.67	6.52	0	104	85	76	68	77	51	50
6	1400/20/45	8	5.53	15.6	6.52	0	39	94	75	73	74	51	49
6	1400/20/45	9	7.8	7.8	6.52	0	104	91	74	67	76	51	50
6	1400/20/45	10	1.42	7.8	6.67	0	143	68	74	62	75	49	49

Table 5: Computational results of the mask models for patient configurations $1 - 6$

C-ID	Patient Config.	Run	objective value/ deviation ω			# unsuc. appointment requests $d_w^r(\cdot)$			# regular slots $\sum_{k\in\mathcal{K}} n_\mu(r,k)$			# chronic slots $\sum_{k\in\mathcal{K}} n_\mu(c,k)$	
			Det-F	Rob-F	RobM-F	Det-F	Rob-F	RobM-F	Det-F	Rob-F	RobM-F	Det-F	Rob(M)-F
7	1600/15/40	1	7.09	15.6	6.81	2	78	145	89	84	82	51	50
7	1600/15/40	2	7.8	9.64	5.96	0	143	130	89	78	86	49	51
7	1600/15/40	3	6.38	6.38	6.24	1	169	104	90	77	89	51	51
7	1600/15/40	4	4.25	12.05	6.24	2	52	96	85	84	87	52	50
7	1600/15/40	5	1.84	7.8	6.24	2	169	110	86	77	91	52	51
7	1600/15/40	6	1.84	7.8	6.24	0	143	92	90	79	90	50	50
7	1600/15/40	7	6.38	11.35	6.95	0	91	82	88	82	88	51	51
7	1600/15/40	8	7.8	9.64	6.24	2	65	109	89	86	90	50	50
7	1600/15/40	9	1.84	7.8	6.38	2	143	94	88	78	88	51	50
7	1600/15/40	10	6.38	7.8	6.38	0	156	92	87	78	90	51	50
8	1600/18/40	1	6.24	7.09	7.09	0	156	139	88	76	85	51	50
8	1600/18/40	2	7.8	15.6	6.24	1	130	121	86	77	85	49	50
8	1600/18/40	3	6.38	7.8	7.09	0	130	91	87	77	85	52	50
8	1600/18/40	4	1.84	10.64	6.38	1	104	89	85	77	84	52	50
8	1600/18/40	5	7.09	7.8	6.38	0	182	106	87	73	92	52	50
8	1600/18/40	6	7.8	7.8	6.24	0	143	103	87	76	91	50	50
8	1600/18/40	7	7.8	7.8	6.95	1	130	80	86	77	88	51	51
8	1600/18/40	8	1.84	16.31	7.09	1	39	103	87	86	87	49	50
8	1600/18/40	9	6.38	7.8	7.09	0	169	87	85	73	83	51	51
8	1600/18/40	10	7.8	7.8	6.24	0	143	91	87	76	84	51	50
9	1600/20/40	1	1.84	8.51	7.09	0	104	120	84	78	86	51	50
9	1600/20/40	2	4.25	10.64	6.38	0	117	106	84	76	82	49	50
9	1600/20/40	3	6.38	6.38	7.09	0	169	88	86	73	85	50	51
9	1600/20/40	4	7.8	12.05	6.95	0	39	110	84	81	83	51	50
9	1600/20/40	5	6.38	7.8	6.95	0	169	111	85	72	89	52	50
9	1600/20/40	6	7.8	7.8	6.38	0	169	114	84	72	87	50	50
9	1600/20/40	7	6.38	11.35	6.95	0	91	103	85	78	85	50	51
9	1600/20/40	8	1.84	17.44	6.1	0	26	117	86	84	84	49	50
9	1600/20/40	9	1.84	7.8	6.52	0	195	80	84	69	85	51	51
9	1600/20/40	10	6.38	7.8	6.38	0	143	84	85	73	85	52	50
10	1600/15/45	1	7.8	20.71	6.24	2	39	133	87	85	87	57	57
10	1600/15/45	2	6.24	12.91	6.95	2	39	114	85	84	82	55	56
10	1600/15/45	3	5.11	19.43	5.96	1	26	131	86	85	82	55	56
10	1600/15/45	4	6.38	23.4	7.09	1	65	136	88	85	89	57	57
10	1600/15/45	5	6.38	17.44	6.24	2	65	127	84	80	81	57	57
10	1600/15/45	6	7.8	27.23	7.09	2	26	125	87	87	87	57	56
10	1600/15/45	7	6.38	21.98	7.09	1	52	138	88	84	85	56	57
10	1600/15/45	8	7.8	7.8	6.95	3	195	138	87	74	83	57	57
10	1600/15/45	9	6.38	17.73	7.09	1	52	120	88	86	88	56	57
10	1600/15/45	10	6.24	12.91	6.38	1	78	111	87	81	83	55	56
11	1600/18/45	1	6.24	14.04	6.1	1	65	110	84	80	83	56	56
11	1600/18/45	2	6.38	6.38	7.09	1	130	122	84	74	82	55	57
11	1600/18/45	3	6.38	28.51	6.24	0	0	138	84	83	85	55	57
11	1600/18/45	4	6.38	23.4	6.38	1	52	151	86	84	85	57	57
11	1600/18/45	5	6.38	23.4	6.95	2	52	168	81	79	74	57	57
11	1600/18/45	6	0.57	29.78	6.38	2	52	139	84	82	82	58	56
11	1600/18/45	7	6.38	27.23	6.38	1	52	130	85	82	81	56	56
11	1600/18/45	8	6.38	15.6	6.38	2	143	165	83	75	77	57	57
11	1600/18/45	9	7.09	5.11	5.96	1	143	152	83	75	79	57	57
11	1600/18/45	10	5.11	14.04	6.95	1	52	111	85	80	84	55	56
12	1600/20/45	1	7.09	21.84	6.24	1	39	141	81	80	80	57	56
12	1600/20/45	2	5.11	12.91	7.09	0	52	102	82	79	79	55	56
12	1600/20/45	3	5.11	28.51	6.38	0	0	145	82	81	74	55	57
12	1600/20/45	4	6.38	21.98	7.09	0	26	132	85	84	84	56	56
12	1600/20/45	5	1.84	16.31	7.09	2	52	148	80	78	77	57	57
12	1600/20/45	6	7.8	28.51	7.09	0	13	122	83	82	79	58	56
12	1600/20/45	7	7.8	20.71	6.38	1	52	144	84	79	80	56	56
12	1600/20/45	8	6.38	19.43	6.38	1	65	148	82	78	78	57	57
12	1600/20/45	9	5.11	20.71	6.38	1	39	104	84	81	81	56	56
12	1600/20/45	10	5.11	12.91	7.09	0	78	109	82	76	80	55	56

Table 6: Computational results of the mask models for patient configurations $7 - 12$

C-ID	Patient Config.	Run	objective value/deviation ω			# unsuc. appointment requests $d_w^r(\cdot)$			# regular slots $\sum\limits_{k\in\mathcal{K}} n_\mu(r,k)$			# chronic slots $\sum\limits_{k\in\mathcal{K}} n_\mu(c,k)$	
			Det-F	Rob-F	RobM-F	Det-F	Rob-F	RobM-F	Det-F	Rob-F	RobM-F	Det-F	Rob(M)-F
13	2000/15/40	1	5.39	34.75	6.52	20	260	292	83	83	84	63	63
13	2000/15/40	2	5.67	14.61	6.67	19	286	285	82	79	83	65	63
13	2000/15/40	3	5.67	14.89	5.39	17	312	299	87	79	84	60	63
13	2000/15/40	4	4.68	22.69	6.38	21	299	297	84	82	86	64	62
13	2000/15/40	5	4.96	38.86	5.81	19	273	312	85	82	87	62	63
13	2000/15/40	6	7.09	21.98	6.52	19	260	297	83	82	83	63	62
13	2000/15/40	7	7.09	26.95	6.52	19	286	301	83	80	83	63	63
13	2000/15/40	8	7.09	16.88	6.38	19	260	270	84	83	86	63	62
13	2000/15/40	9	5.39	25.81	6.52	20	273	298	83	82	83	64	63
13	2000/15/40	10	4.96	18.01	6.38	17	286	259	84	81	85	63	63
14	2000/18/40	1	5.81	34.75	6.38	20	234	258	82	82	83	65	63
14	2000/18/40	2	5.67	15.46	5.81	17	247	262	82	80	81	64	63
14	2000/18/40	3	4.68	18.01	6.38	16	260	250	86	80	85	62	63
14	2000/18/40	4	7.09	29.78	6.67	17	247	266	85	83	85	63	62
14	2000/18/40	5	3.55	38.86	5.39	17	247	288	83	81	86	62	63
14	2000/18/40	6	7.09	20.28	6.52	16	260	268	83	81	84	63	63
14	2000/18/40	7	4.68	19.15	6.67	19	247	273	81	81	82	64	63
14	2000/18/40	8	5.39	6.38	6.52	18	260	257	84	81	84	62	62
14	2000/18/40	9	4.68	22.69	6.52	18	247	293	84	83	85	64	63
14	2000/18/40	10	4.96	25.81	6.38	17	221	242	84	84	85	63	63
15	2000/20/40	1	4.68	23.4	6.38	16	208	230	81	82	84	65	62
15	2000/20/40	2	7.09	14.61	6.52	15	234	249	83	79	81	64	63
15	2000/20/40	3	7.09	11.35	6.38	15	260	256	86	78	82	61	64
15	2000/20/40	4	5.81	25.81	6.38	18	260	269	83	81	85	64	62
15	2000/20/40	5	5.67	26.24	4.96	17	234	270	82	81	85	64	63
15	2000/20/40	6	7.09	14.89	6.52	15	234	262	83	80	79	63	63
15	2000/20/40	7	5.81	29.78	6.52	16	221	258	82	81	83	63	63
15	2000/20/40	8	5.39	18.01	6.81	16	247	267	84	80	82	62	63
15	2000/20/40	9	5.39	34.75	6.67	17	208	258	83	84	86	64	63
15	2000/20/40	10	4.68	24.68	6.38	16	221	245	84	82	82	63	63
16	2000/15/45	1	7.8	41.55	7.09	19	247	292	78	78	77	72	71
16	2000/15/45	2	5.81	21.41	11.2	21	286	305	76	75	78	71	71
16	2000/15/45	3	7.8	41.13	11.49	21	221	287	78	80	81	71	71
16	2000/15/45	4	7.8	40.42	11.49	20	273	304	77	76	77	72	71
16	2000/15/45	5	2.13	17.73	6.52	21	247	277	76	78	79	72	70
16	2000/15/45	6	7.8	15.6	6.95	19	286	304	78	77	79	71	70
16	2000/15/45	7	7.8	30.92	7.09	20	273	315	78	76	76	69	71
16	2000/15/45	8	7.8	36.02	7.09	19	273	296	78	77	77	71	71
16	2000/15/45	9	4.82	36.02	14.04	21	299	311	77	75	78	71	71
16	2000/15/45	10	6.38	29.78	6.52	21	299	308	76	74	75	71	71
17	2000/18/45	1	7.8	42.55	7.37	17	234	284	78	78	78	72	71
17	2000/18/45	2	6.38	21.98	9.93	19	286	304	77	74	74	70	71
17	2000/18/45	3	4.82	46.8	9.64	21	208	274	77	80	83	71	71
17	2000/18/45	4	2.13	40.42	12.05	20	260	307	75	75	75	72	71
17	2000/18/45	5	7.8	21.98	6.81	18	221	256	76	78	78	72	70
17	2000/18/45	6	4.82	23.4	7.52	21	286	297	76	75	78	72	71
17	2000/18/45	7	6.38	24.82	6.81	19	273	299	77	75	76	69	71
17	2000/18/45	8	7.8	31.2	6.95	18	260	294	79	77	77	70	70
17	2000/18/45	9	7.8	28.22	11.49	19	286	306	77	74	76	70	71
17	2000/18/45	10	2.13	29.78	10.92	21	247	269	75	76	77	72	71
18	2000/20/45	1	4.82	33.75	6.38	17	208	272	78	78	76	72	71
18	2000/20/45	2	5.81	21.98	12.05	17	273	265	78	73	76	69	71
18	2000/20/45	3	7.8	41.13	10.35	18	182	256	76	80	83	71	71
18	2000/20/45	4	7.8	40.42	15.17	18	247	268	76	75	81	71	71
18	2000/20/45	5	7.8	17.73	7.09	18	208	243	76	78	78	72	70
18	2000/20/45	6	5.67	19.15	6.95	19	273	268	76	75	79	72	71
18	2000/20/45	7	7.8	25.53	8.51	20	260	297	76	74	75	71	71
18	2000/20/45	8	2.13	28.22	7.09	17	286	289	78	74	76	69	71
18	2000/20/45	9	4.82	29.07	14.75	19	286	302	76	74	77	70	71
18	2000/20/45	10	5.81	37.01	13.19	18	208	239	74	77	77	72	71

Table 7: Computational results of the mask models for patient configurations $13-18$

C-ID	Config.	IBFI	AA	AM	HM	2B	M	RM-52	RM-13	MM-52	MM-13
1	1400/15/40	59.43	9.31	9.33	3.28	5.07	2.05	2.04	1.81	1.27	0.98
2	1400/18/40	45.11	9.33	13.38	4.08	3.91	1.86	2.11	1.33	1.17	1.96
3	1400/20/40	58.82	9.87	11.96	2.01	5.28	1.68	1.6	2.28	0.83	1.69
4	1400/15/45	53.38	10.5	12.71	4.1	4.65	2.88	2.51	1.52	1.64	1.53
5	1400/18/45	50.49	10.04	8.73	4.27	5.04	2.24	2.54	2.39	3.17	1.8
6	1400/20/45	53.88	9.63	12.43	3.94	4.19	2.68	2.52	1.78	2.02	1.89
7	1600/15/40	100.65	18.04	21.48	9.68	10.39	4.8	6.92	5.47	5.82	5.67
8	1600/18/40	73.42	22.05	18.49	11.54	13.25	7.73	9	7.37	5.8	8.58
9	1600/20/40	97.9	19.67	23.84	10.57	12.64	6.37	11.05	6.3	9.2	6.27
10	1600/15/45	90.92	18.73	21.65	12.47	13.59	10.13	9.66	11.57	7.83	10.85
11	1600/18/45	96.96	23.17	21.48	14.46	17.23	11.58	10	10.58	9.51	8.05
12	1600/20/45	106.76	22.34	25	17.5	12.13	10.63	13.09	11.14	5.17	8.92
13	2000/15/40	257.01	68.46	67.54	67.51	53.61	53.46	48.89	51.12	56.07	52.32
14	2000/18/40	238.15	74.33	69.82	68.05	59.23	50.63	48.24	50.23	60.84	48.47
15	2000/20/40	227.15	76.88	65.48	72.86	53.47	52.05	53.72	53.46	51.89	45.22
16	2000/15/45	242.28	85.6	80.73	83.49	64.6	65.97	72.86	61.79	62.6	59.45
17	2000/18/45	230.46	86.4	74.72	77.64	77.15	67.71	67.32	60.04	64.66	65.12
18	2000/20/45	247.95	79.36	79.37	76.95	64.7	71.22	63.24	62.71	61.89	57.73

Table 8: Average overtime of the PCP among the ten runs

C-ID	Config.	IBFI	AA	AM	HM	2B	M	RM-52	RM-13	MM-52	MM-13
1	1400/15/40	493.98	492.26	847.05	602.85	425.84	391.59	390.48	404.27	397.6	402.49
2	1400/18/40	516.51	480.46	824.52	583.96	416.16	390.62	409.91	387.45	392.84	397.65
3	1400/20/40	516.48	480.49	832.95	567.63	423.71	398.27	392.75	401.54	393.65	386.67
4	1400/15/45	492.17	462.7	782.85	566.4	395.8	366.98	376.37	374.37	372	367.86
5	1400/18/45	481.35	464.48	771.33	538.41	386.08	365.15	376.66	374.3	370.52	367.46
6	1400/20/45	485.01	444.78	770.05	528.41	381.47	371.14	361.77	382.39	370.07	368.61
7	1600/15/40	375.92	362.27	622.13	433.88	292.27	280.89	277.53	273.45	258.72	265.81
8	1600/18/40	376.54	349.4	622.37	437.73	285.24	270.78	271.72	272.38	271.97	257.19
9	1600/20/40	372.02	344.86	615.21	427.01	296.2	268.28	280.94	269.57	264.3	268.33
10	1600/15/45	337.32	314.56	584.57	393.52	268.51	263.69	267.45	258.6	240.58	250.07
11	1600/18/45	345.3	337.23	561.82	394.51	268.45	264.58	256.87	259.8	241.26	242.31
12	1600/20/45	323.86	325.86	586.08	394.26	275.01	260.96	258.22	254.06	239.98	248.45
13	2000/15/40	115.65	166.94	326.26	246.4	132.41	120.31	107.06	109.46	104.84	98.88
14	2000/18/40	115.14	167.14	324.67	217.99	120.01	129.02	113.47	116.95	106.66	110.29
15	2000/20/40	114.43	160.84	327.18	251.75	135.78	124.38	119.52	109.33	99.78	107.21
16	2000/15/45	81.36	145.07	280.86	217.63	118.66	101.68	90.83	103.01	90.5	106.18
17	2000/18/45	96.07	153.06	273.15	215.01	111.84	98.47	98	102.32	81.95	90.34
18	2000/20/45	99.88	135.05	293.59	208.47	111.9	96.36	106.29	100.57	97.26	97.02

Table 9: Average idle time of the PCP among the ten runs

C-ID	Config.	IBFI	AA	AM	HM	2B	M	RM-52	RM-13	MM-52	MM-13
1	1400/15/40	0.65	0.59	0.62	0.55	0.54	0.49	0.46	0.38	0.49	0.46
2	1400/18/40	0.65	0.61	0.62	0.53	0.51	0.5	0.5	0.41	0.48	0.46
3	1400/20/40	0.62	0.58	0.62	0.54	0.55	0.51	0.72	0.58	0.58	0.45
4	1400/15/45	0.66	0.56	0.6	0.52	0.49	0.48	0.52	0.55	0.4	0.4
5	1400/18/45	0.63	0.54	0.61	0.51	0.51	0.48	0.56	0.41	0.4	0.42
6	1400/20/45	0.64	0.57	0.62	0.48	0.49	0.44	0.52	0.63	0.44	0.38
7	1600/15/40	0.6	0.54	0.63	0.5	0.49	0.54	0.39	0.4	0.44	0.51
8	1600/18/40	0.62	0.55	0.63	0.5	0.52	0.56	0.48	0.46	0.41	0.4
9	1600/20/40	0.59	0.57	0.61	0.5	0.49	0.55	0.53	0.46	0.41	0.42
10	1600/15/45	0.6	0.53	0.59	0.53	0.51	0.54	0.53	0.42	0.45	0.5
11	1600/18/45	0.6	0.5	0.59	0.49	0.52	0.58	0.53	0.43	0.45	0.51
12	1600/20/45	0.59	0.57	0.59	0.49	0.5	0.55	0.38	0.58	0.45	0.48
13	2000/15/40	0.65	0.53	0.54	0.49	0.46	0.47	0.35	0.39	0.45	0.42
14	2000/18/40	0.62	0.52	0.55	0.47	0.47	0.52	0.43	0.52	0.48	0.44
15	2000/20/40	0.59	0.51	0.54	0.47	0.44	0.44	0.41	0.57	0.49	0.48
16	2000/15/45	0.55	0.5	0.53	0.46	0.44	0.5	0.43	0.64	0.41	0.41
17	2000/18/45	0.57	0.47	0.52	0.44	0.46	0.49	0.48	0.66	0.38	0.47
18	2000/20/45	0.55	0.53	0.54	0.45	0.46	0.52	0.45	0.47	0.43	0.41

Table 10: Average maximum deviation of the actual from the optimal PCP's workload among the ten runs

C-ID	Config.	IBFI	AA	AM	HM	2B	M	RM-52	RM-13	MM-52	MM-13
1	1400/15/40	1.11	5.1	2.41	6.29	2.2	1.89	2.03	2.24	2.31	2.23
2	1400/18/40	1.11	5.03	2.35	6.14	2.13	1.96	2.06	2.25	2.37	2.24
3	1400/20/40	1.1	5.05	2.3	6.06	2.09	1.95	2.1	2.23	2.32	2.18
4	1400/15/45	1.13	6.29	2.55	4.53	2.31	2	2.04	2.28	2.34	2.22
5	1400/18/45	1.13	6.31	2.49	4.55	2.26	2.04	2.05	2.23	2.29	2.16
6	1400/20/45	1.13	6.3	2.44	4.6	2.21	2.1	2.02	2.23	2.32	2.28
7	1600/15/40	1.15	6.43	2.82	4.28	2.59	2.04	2.03	2.22	2.27	2.25
8	1600/18/40	1.15	6.36	2.75	4.33	2.52	2.01	2.07	2.19	2.34	2.22
9	1600/20/40	1.14	6.37	2.69	4.32	2.48	1.97	2.05	2.21	2.34	2.23
10	1600/15/45	1.2	7.35	2.98	4.86	2.73	2.16	2.16	2.21	2.47	2.36
11	1600/18/45	1.2	7.33	2.92	4.8	2.67	2.15	2.13	2.21	2.43	2.31
12	1600/20/45	1.19	7.35	2.87	4.81	2.64	2.16	2.16	2.25	2.36	2.39
13	2000/15/40	1.36	7.74	3.88	6.01	3.48	2.54	2.45	2.54	2.57	2.62
14	2000/18/40	1.33	7.71	3.74	6.02	3.37	2.52	2.36	2.43	2.51	2.48
15	2000/20/40	1.31	7.72	3.66	5.95	3.3	2.5	2.32	2.49	2.42	2.46
16	2000/15/45	1.46	7.93	4.73	7	4.09	2.72	2.57	2.63	2.75	2.65
17	2000/18/45	1.42	7.93	4.6	6.97	3.97	2.69	2.53	2.59	2.71	2.69
18	2000/20/45	1.4	7.94	4.48	6.99	3.9	2.71	2.56	2.56	2.69	2.58

Table 11: Average access time to an appointment for regular patients among the ten runs

C-ID	Config.	IBFI	AA	AM	HM	2B	M	RM-52	RM-13	MM-52	MM-13
1	1400/15/40	1.41	4.71	1.71	2.84	1.52	3	3.09	3.22	3.1	3.3
2	1400/18/40	1.41	4.67	1.71	2.82	1.52	3.02	3.14	3.19	3.17	3.23
3	1400/20/40	1.41	4.69	1.71	2.81	1.53	3.08	3.16	3.09	3.07	3.05
4	1400/15/45	1.4	5.93	1.75	3.32	1.54	3.12	2.97	3.25	3.09	3.14
5	1400/18/45	1.4	5.96	1.75	3.33	1.54	3.15	2.91	3.04	2.95	2.98
6	1400/20/45	1.4	5.96	1.75	3.36	1.55	3.23	2.88	3.07	2.97	3.18
7	1600/15/40	1.4	6.07	1.71	3.44	1.53	3.08	2.88	3.22	3.05	3.22
8	1600/18/40	1.4	6.03	1.71	3.45	1.54	3.01	3	3.02	3.15	3.09
9	1600/20/40	1.4	6.02	1.71	3.48	1.54	3.06	2.98	3.11	3.12	3.21
10	1600/15/45	1.41	7.04	1.78	4.58	1.6	3.08	3.14	3.12	3.23	3.27
11	1600/18/45	1.41	7.05	1.79	4.53	1.6	3.07	3.07	3.05	3.16	3.09
12	1600/20/45	1.4	7.06	1.79	4.51	1.6	3.08	3.05	3.22	3	3.22
13	2000/15/40	1.39	7.34	1.81	5.61	1.62	3.25	3.03	3.11	3.07	3.15
14	2000/18/40	1.39	7.33	1.81	5.6	1.62	3.28	2.92	3	2.99	3
15	2000/20/40	1.39	7.35	1.82	5.56	1.62	3.28	2.89	3.19	2.89	2.97
16	2000/15/45	1.42	7.5	1.97	6.57	1.77	3.27	2.84	3.02	2.86	2.87
17	2000/18/45	1.42	7.48	1.97	6.56	1.79	3.27	2.86	3.04	2.94	3.04
18	2000/20/45	1.42	7.5	1.96	6.58	1.79	3.35	3.03	3.05	2.95	2.88

Table 12: Average access time to an appointment for chronic patients among the ten runs

C-ID	Config.	IBFI	AA	AM	HM	2B	M	RM-52	RM-13	MM-52	MM-13
1	1400/15/40	988.1	5172.7	2940.8	4872.7	2763.5	1346.1	1488.2	1729.7	1358.4	1353.7
2	1400/18/40	942.5	4985.8	2756.1	4692.2	2579.4	1398.8	1422.8	1693.3	1307.4	1300.9
3	1400/20/40	916.1	4869.9	2643.6	4574.2	2465.3	1284.7	1422.5	1662.8	1233.5	1311
4	1400/15/45	985.2	5123.4	3155.2	5023.2	2979.5	1310.6	1468.2	1675.7	1392.1	1371.8
5	1400/18/45	941.3	4946.5	2983.1	4845.7	2802.1	1316.9	1437.6	1669.5	1328.5	1273.6
6	1400/20/45	912.4	4828.2	2869.3	4728.3	2690	1289.9	1384.7	1578.1	1295.4	1247.2
7	1600/15/40	1209.9	5927.5	3975.1	5857.1	3793.6	1716.6	1805.1	1915.7	1489.2	1611.4
8	1600/18/40	1150.2	5722.3	3772.1	5646.8	3590.3	1639.8	1712.3	1910.1	1529.6	1529.1
9	1600/20/40	1113.3	5581.3	3637.7	5514.1	3456.8	1465.5	1631.9	1844	1504.5	1418.7
10	1600/15/45	1261.8	5889.8	4220.3	5846.4	4045.7	1868.1	1732.1	1875.7	1701.5	1706.1
11	1600/18/45	1201.1	5687.4	4023.5	5647	3848	1761.8	1666.9	1851.2	1596.7	1617.3
12	1600/20/45	1161	5551.8	3891.2	5510	3715.7	1710.6	1662.8	1742	1523.8	1630.7
13	2000/15/40	1991.4	7429.4	5980.5	7384.4	5813.2	3026.5	2978.2	3082.6	2659.4	2921.7
14	2000/18/40	1851.8	7168.9	5725.9	7119.1	5557.5	2853.7	2748.4	2836.4	2482.1	2708.3
15	2000/20/40	1769.4	6996.6	5561.5	6948.2	5393.8	2744.2	2620.8	2735	2334.1	2627.8
16	2000/15/45	2219.3	7460.5	6358.9	7414.3	6202.7	3339.8	3385.9	3314.4	3101.8	3252.2
17	2000/18/45	2055.9	7203.9	6118.4	7159.2	5953.2	3160.1	3128	3121.1	2839	3035.2
18	2000/20/45	1953.9	7031.1	5956.3	6991.1	5791.7	3025.2	2979.3	2976.2	2719	2837.8

Table 13: Average total number of patient with an unsuccessful appointment request among the ten runs

C-ID	Config.	IBFI	AA	AM	HM	2B	M	RM-52	RM-13	MM-52	MM-13
1	1400/15/40	94.8	9.4	25.7	3.4	6.8	0.4	0.8	1.3	0	0
2	1400/18/40	95.4	9.8	26.1	5.9	4.8	0.1	0.5	0.6	0.3	0.2
3	1400/20/40	101.3	8.1	28.7	2	5.7	0.2	0.6	0.6	0.3	0.3
4	1400/15/45	88	10.6	22.5	4.2	5.9	0.3	0.5	0.2	0.2	0.2
5	1400/18/45	91.4	9.3	21.4	4.3	7.3	0.5	0.5	0.5	0.2	0
6	1400/20/45	94.7	9.9	21.6	3.1	5.7	0.7	0.1	0.9	0	0
7	1600/15/40	163.2	29.3	55.5	16.5	23.7	3	3.2	2.2	1.7	1.7
8	1600/18/40	169.8	36.6	56.3	18.6	25.3	3.3	4.8	4	2.1	2.4
9	1600/20/40	176	30.5	54.7	19.6	24.5	2.1	4.1	3.3	3.5	2.6
10	1600/15/45	160.9	34	58.4	22.1	27.1	7.8	3.6	5.1	2.3	2.7
11	1600/18/45	172	41.5	55.6	25.6	26.5	6.5	5.7	4.7	3.4	3.4
12	1600/20/45	175.5	43	61.3	23.8	28.8	6.7	3.8	5	4.3	4.6
13	2000/15/40	350.4	264.2	263.9	209.6	218.4	99.4	82.5	68.4	76.6	60.4
14	2000/18/40	364.5	268.2	273.3	222	212.3	104.8	82.8	74.1	75	73.5
15	2000/20/40	370.2	263.5	271.2	215.4	213.8	100.8	77.5	80.3	72.3	73.3
16	2000/15/45	378.1	319.9	305.2	267.9	253.3	152.7	123.6	120.8	102.6	104.5
17	2000/18/45	386.2	315.1	304.7	276.9	250.3	149.3	119.7	126.8	105.4	109.3
18	2000/20/45	399.7	304.1	303.2	280.3	259.1	152	119.9	114.1	108	97.4

Table 14: Average total number of rejected walk-ins among the ten runs

C-ID	Config.	IBFI	AA	AM	HM	2B	M	RM-52	RM-13	MM-52	MM-13
1	1400/15/40	54.9	8	19.7	2.5	4.9	0.1	0.3	0.7	0	0
2	1400/18/40	51.3	7.6	19.9	4.3	3.3	0.1	0.4	0.4	0.2	0.2
3	1400/20/40	51.3	6.9	20.2	1.7	3.4	0.1	0.3	0.5	0.2	0.2
4	1400/15/45	53.1	7.7	18.1	3.7	5.3	0.3	0.3	0.1	0	0.2
5	1400/18/45	50	6.9	16.6	3.5	5.4	0.2	0.3	0.4	0.2	0
6	1400/20/45	49.7	7.2	16	2.9	3.6	0.6	0.1	0.7	0	0
7	1600/15/40	107	22.2	45.6	14	18.8	1.7	1.6	1.3	0.6	1.2
8	1600/18/40	100.1	28.6	42.5	14.7	19.3	1.4	3	2.1	0.5	0.8
9	1600/20/40	100.2	22.8	41	14.8	16.9	0.8	2.1	1.6	2	0.9
10	1600/15/45	108.7	27.5	46.9	17.6	21.9	5.2	1.8	3	1.4	1.5
11	1600/18/45	107.1	31.5	44.1	18.8	20.2	4.1	2.9	3.3	1.6	2.2
12	1600/20/45	105.4	31.5	46.6	16.9	20.2	4	2.1	2.6	1.9	2.6
13	2000/15/40	247	200.8	217.8	162.4	181.5	70.5	55.7	47.8	47.6	38.6
14	2000/18/40	237.6	196.7	217.2	164.8	168.8	69.4	51.4	45	42	47.1
15	2000/20/40	228.9	183.4	210.9	161	161.9	63.5	47.3	48.3	37.3	41.7
16	2000/15/45	269	232.1	255.2	198.4	210.4	113.8	87.8	85	65	74.9
17	2000/18/45	254.4	223.6	243.5	200.9	193.4	104.8	79.4	84.6	64.6	71.9
18	2000/20/45	251.7	209.8	234.7	199	198.4	97.5	72.8	73.1	60.5	59.3

Table 15: Average total number of rejected walk-ins who previously had an unsuccessful appointment request among the ten runs

C-ID	Config.	IBFI	AA	AM	HM	2B	M	RM-52	RM-13	MM-52	MM-13
1	1400/15/40	5.84	3.54	3.06	3.42	5.67	6.32	6.29	6.27	6.18	6.19
2	1400/18/40	5.84	3.39	3.09	3.6	5.84	6.17	6.04	6.06	6.38	6.26
3	1400/20/40	6	3.4	3.18	3.45	5.89	6.14	6.14	6.17	6.06	6.24
4	1400/15/45	5.91	3.4	3.17	3.41	5.72	6.36	6.36	6.12	6.34	6.11
5	1400/18/45	5.97	3.53	3.25	3.33	5.8	6.46	6.21	6.21	6.38	6.3
6	1400/20/45	5.91	3.64	3.21	3.46	5.76	6.25	6.19	6.26	6.2	6.42
7	1600/15/40	6.16	3.51	3.48	3.54	5.87	6.32	6.49	6.37	6.45	6.44
8	1600/18/40	6.15	3.64	3.41	3.31	5.69	6.32	6.64	6.28	6.26	6.61
9	1600/20/40	6.22	3.62	3.39	3.49	5.74	6.52	6.59	6.6	6.49	6.52
10	1600/15/45	6.33	3.55	3.48	3.46	5.8	6.42	6.42	6.62	6.3	6.56
11	1600/18/45	6.5	3.7	3.47	3.38	5.84	6.43	6.59	6.38	6.52	6.48
12	1600/20/45	6.54	3.59	3.4	3.53	5.81	6.55	6.54	6.72	6.43	6.4
13	2000/15/40	6.71	3.52	3.6	3.49	5.74	6.67	6.62	6.47	6.68	6.59
14	2000/18/40	6.71	3.66	3.63	3.48	5.71	6.5	6.42	6.48	6.58	6.51
15	2000/20/40	6.67	3.52	3.64	3.4	5.61	6.52	6.54	6.62	6.42	6.39
16	2000/15/45	6.72	3.59	3.76	3.33	5.71	6.56	6.42	6.43	6.51	6.4
17	2000/18/45	6.73	3.38	3.67	3.6	5.64	6.32	6.52	6.45	6.46	6.37
18	2000/20/45	6.82	3.43	3.71	3.48	5.7	6.52	6.4	6.57	6.52	6.46

Table 16: Average waiting time for treatment within the practice for patients with appointments among the ten runs

C-ID	Config.	IBFI	AA	AM	HM	2B	M	RM-52	RM-13	MM-52	MM-13
1	1400/15/40	101.91	29.28	46.96	40.54	67.01	65.88	60.77	60.13	65.85	64.05
2	1400/18/40	97.06	29.45	47.55	40.9	67.17	64.24	57.99	59.1	64.57	63.73
3	1400/20/40	95.82	29.76	47.11	40.44	67.48	63.23	58.42	58.81	62.87	63.48
4	1400/15/45	100.76	30.26	45.9	40.97	65.98	67.92	62.27	60.87	65	66.24
5	1400/18/45	96.3	30.11	45.62	40.53	66.4	67.13	62.65	60.73	66.18	64.48
6	1400/20/45	94.61	29.94	45.91	41.03	66.51	65.43	62.88	60.18	63.19	64.01
7	1600/15/40	108.9	36.07	51.26	47.66	72.03	75.93	70.65	68.02	77.24	73.94
8	1600/18/40	103.64	36.24	50.74	47.16	71.81	74.86	70.95	67.96	76.22	73.98
9	1600/20/40	102.74	36.25	51.11	47.78	71.35	72.95	71.29	68.87	73.89	72.95
10	1600/15/45	110	37.1	51.17	48.98	71.99	78.96	75.72	73.77	80.16	77.95
11	1600/18/45	106.28	37.63	51.46	48.5	72.73	76.9	74.58	73.28	78.87	76.21
12	1600/20/45	104.69	36.99	50.99	48.41	71.54	75.77	73.67	73.2	78.57	75.52
13	2000/15/40	121.75	51.22	62.63	62.81	84.51	93.31	91.24	89.86	100.14	94.17
14	2000/18/40	119.57	51.52	63.25	63.09	84.93	92.34	90.03	90.12	98.92	93.97
15	2000/20/40	117.72	51.6	62.64	63.02	84.52	91.72	90.32	90.16	97.58	93.32
16	2000/15/45	120.79	53.55	64.8	64.85	85.86	97.19	93.28	95.23	100.73	97.88
17	2000/18/45	118.97	53.59	64.16	65.28	86.21	96.06	93.19	95.76	100.12	98.11
18	2000/20/45	118.51	53.14	64.61	64.81	86.17	96.26	93.04	94.83	99.65	97.24

Table 17: Average waiting time for treatment within the practice for walk-ins among the ten runs

Acknowledgements